Geodynamics, geophysical and geochemical observations, and the role of CO2 degassing in the Apennines

F. Di Luccio, M. Palano, G. Chiodini, L. Cucci, C. Piromallo, F. Sparacino, G. Ventura, L. Improta, C. Cardellini, P. Persaud, L. Pizzino, G. Calderoni, C. Castellano, G. Cianchini, S. Cianetti, D. Cinti, P. Cusano, P. De Gori, A. De Santis, P. Del Gaudio, G. Diaferia, A. Esposito, D. Galluzzo, A. Galvani, A. Gasparini, G. Gaudiosi, A. Gervasi, C. Giunchi, M. La Rocca, G. Milano, S. Morabito, L. Nardone, M. Orlando, S. Petrosino, D. Piccinini, G. Pietrantonio, A. Piscini, P. Roselli, D. Sabbagh, A. Sciarra, L. Scognamiglio, V. Sepe, A. Tertulliani, R. Tondi, L. Valoroso, N. Voltattorni, L. Zuccarello

PII: S0012-8252(22)00320-8

DOI: https://doi.org/10.1016/j.earscirev.2022.104236

Reference: EARTH 104236

To appear in: *Earth-Science Reviews*

Received date: 31 March 2022

Revised date: 17 October 2022

Accepted date: 24 October 2022

Please cite this article as: F. Di Luccio, M. Palano, G. Chiodini, et al., Geodynamics, geophysical and geochemical observations, and the role of CO2 degassing in the Apennines, *Earth-Science Reviews* (2022), https://doi.org/10.1016/j.earscirev.2022.104236

Geodynamics, geophysical and geochemical observations, and the role of CO_2 degassing in the Apennines

F. Di Luccio[1], M. Palano[2], G. Chiodini[3], L. Cucci[1], C. Piromallo[1], F. Sparacino[2], G. Ventura[1,4], L. Improta[5], C. Cardellini[6,3], P. Persaud[7], L. Pizzino[1], G. Calderoni[1], C. Castellano[1], G. Cianchini[8], S. Cianetti[9], D. Cinti[1], P. Cusano[10], P. De Gori[5], A. De Santis[8], P. Del Gaudio[5], G. Diaferia[5], A. Esposito[5], D. Galluzzo[10], A. Galvani[5], A. Gasparini[1], G. Gaudiosi[10], A. Gervasi[5], C. Giunchi[9], M. La Rocca[11], G. Milano[10], S. Morabito[10], L. Nardone[10], M. Orlando[2], S. Petrosino[10], D. Piccinini[9], G. Pietrantonio[5], A. Piscini[5], P. Roselli[1], D. Sabbagh[8], A. Sciarra[1], L. Scognamiglio[5], V. Sepe[5], A. Tertulliani[1], R. Tondi[3], L. Valoroso[5], N. Voltattorni[1], L. Zuccarello[9]

[1]Istituto Nazionale di Geofisica e Vulcanologia, Roma1, Via di Vigna Murata 605, 00143, Rome, ITALY

[2]Istituto Nazionale di Geofisica e Vulcanologia, Osservatorio Etneo, Piazza Roma 2, 95125, Catania, ITALY

[3]Istituto Nazionale di Geofisica e Vulcanologia, Bologna, Via Franceschini 31, 40128, Bologna, ITALY

[4]Istituto per lo studio degli impatti Antropici e Sostenibilità in ambiente marino (IAS) - CNR, via del Mare 3, Torretta Granitola, 91021, Trapani, ITALY

[5]Istituto Nazionale di Geofisica e Vulcanologia, Osservatorio Nazionale Terremoti, Via di Vigna Murata 605, 00143, Rome, ITALY

[6]Università di Perugia, Dipartimento di Fisica e Geologia, via Alessandro Pascoli snc, 06123, Perugia, ITALY

[7]Louisiana State University, Department of Geology and Geophysics, E235 Howe-Russell-Kniffen, Baton Rouge, LA 70803, USA

[8]Istituto Nazionale di Geofisica e Vulcanologia, Roma2, Via di Vigna Murata 605, 00143, Rome, ITALY

[9]Istituto Nazionale di Geofisica e Vulcanologia, Pisa, Via Cesare Battisti 53, 56125, Pisa, ITALY

[10]Istituto Nazionale di Geofisica e Vulcanologia, Osservatorio Vesuviano, via Diocleziano, 328, 80124, Napoli, ITALY

[11]Università della Calabria, Dipartimento di Biologia, Ecologia e Scienze della Terra, via Pietro Bucci 87036, Arcavacata di Rende, Cosenza, ITALY

Corresponding authors:

Mimmo Palano
Istituto Nazionale di Geofisica e Vulcanologia
Piazza Roma 2, Catania - Italy
Ph. +39-095-7165812
mimmo.palano@ingv.it

Francesca Di Luccio
Istituto Nazionale di Geofisica e Vulcanologia
via di Vigna Murata 605, Rome - Italy
Ph. +39-06-51860561
francesca.diluccio@ingv.it

Highlights

- Multidisciplinary datasets are key to understand the fluid-seismicity interplay
- Joint interpretation of CO_2 distribution and geophysical data in the Apennines
- Deep-origin CO_2 derives from the melting of carbonate-rich lithologies
- Mantle wedge modulates the slab thermal structure, rheology and melting
- New maps of seismogenic thickness, geodetic velocities and strains for the Apennines

Abstract

An accurate survey of old and new datasets allowed us to probe the nature and role of fluids in the seismogenic processes of the Apennines mountain range in Italy. New datasets include the

1985-2021 instrumented seismicity catalog, the computed seismogenic thickness, and geodetic velocities and strains, whereas data from the literature comprise focal mechanism solutions, CO_2 release, Moho depth, tomographic seismic velocities, heat flow and Bouguer gravity anomalies. Most of the inspected datasets highlight differences between the western and eastern domains of the Apennines, while the transition zone is marked by high geodetic strain, prevailing uplift at the surface and high seismic release, and spatially corresponds with the overlapping Tyrrhenian and Adriatic Mohos. Published tomographic models suggest the presence of a large hot asthenospheric mantle wedge which intrudes beneath the western side of the Apennines and disappears at the southern tip of the southern Apennines. This wedge modulates the thermal structure and rheology of the overlying crust as well as the melting of carbonate-rich sediments of the subducting Adriatic lithosphere. As a result, CO_2-rich fluids of mantle-origin have been recognized in association with the occurrence of destructive seismic sequences in the Apennines. The stretched western domain of the Apennines is characterized by a broad pattern of emissions from CO_2-rich fluids that vanishes beneath the axial belt of the chain, where fluids are instead trapped within crustal overpressurized reservoirs, favoring their involvement in the evolution of destructive seismic sequences in that region. In the Apennines, areas with high mantle He are associated with different degrees of metasomatism of the mantle wedge from north to south. Beneath the chain, the thickness and permeability of the crust control the formation of overpressurized fluid zones at depth and the seismicity is favored by extensional faults that act as high permeability pathways. This multidisciplinary study aims to contribute to our understanding of the fluid-related mechanisms of earthquake preparation, nucleation and evolution encouraging a multiparametric monitoring system of different geophysical and geochemical observables that could lead the creation of a data-constrained and reliable conceptual model of the role of fluids in the preparatory phase of earthquakes in the Apennines.

Keywords: CO_2 Earth degassing, earthquakes, mantle wedge, subduction, Apennines.

1. Introduction

In the last decades, mantle fluid signatures in crustal faulting environments have been recognized worldwide as well as in the Apennines, Italy (Chiodini et al., 2020; Lee et al., 2016; Vannoli et al., 2021; Gunatilake and Miller, 2022). The Earth's crust is almost entirely filled with fluids of different types: the meteoric fluids that circulate in the upper crust, and the mantle-derived volatiles that flow upward within the entire lithosphere. Fluid transfer from the mantle to the crust and fluid movements within the crust occur by hydraulic fracturing, diffusion processes, buoyancy forces and head gradients (Sibson, 1992, 2020; Miller et al., 2004; Shapiro and Dinske, 2009). In tectonically active regions, faults and crustal-scale shear zones are preferential pathways for the upward migration of fluids, due to their high permeability. Fluid flow along high-permeability pathways such as fault-zones can alter both the state of stress and rock strength, therefore favoring fault slip, especially when the crust is critically stressed (Zoback et al., 2002).

Recognition of fault-fluid interactions extends back into mining history when water was identified as the causative agent for vein formation (Agricola, 1556). A qualitative appreciation of the role of fluid pressure in counteracting normal stress during faulting and vein formation was discussed by McKinstry (1948), while the primary role of overpressurized fluids in lowering the strength of thrust faults was identified by Hubbert and Rubey (1959). Evidence of the influence of fluid pressure on fault slip potential has been provided by induced earthquakes either in intraplate regions (e.g., Keranen and Weingarten, 2018), through the direct injection of fluids in boreholes (Healy et al., 1968; Raleigh et al., 1976), or from the filling of large reservoirs (Simpson, 1986). Since then, the availability of large datasets and observations collected in numerous hydrocarbon industry exploration sites and geothermal systems worldwide (among others Keranen et al., 2014; Grigoli et al., 2018) as well as in-situ stimulation experiments performed in underground laboratories (Gischig et al., 2020) have largely proved the importance of fluids in the seismogenic process.

Fluid involvement in the occurrence of natural seismicity is well documented in the preparatory phase of major earthquakes and in the evolution of aftershocks and swarms in space and time (Barnes, 1978; Gold and Soter, 1984; Bräuer et al., 2003; Hainzl, 2003; Ventura et al., 2007; Massin et al., 2013; Miller, 2013; Fischer et al., 2014; Yoshida and Hasegawa, 2018; Chiodini et al., 2020). In this context, spatial correlations between seismicity and mantle-derived fluids have been largely documented worldwide in extensional domains (Irwin and Barnes, 1980; Tamburello et al., 2018).

In the complex framework of the Mediterranean (Fig. 1a) where fragments of continental and oceanic lithosphere interact under the slow African-Eurasian convergence, the seismically active Apennines mountain chain represents a natural laboratory to investigate the interplay between fluids and seismicity. The Apennines (Fig. 1b, c) is a Neogene fold-and-thrust belt that is characterized by NW-SE striking active normal faults that are parallel to the chain axis and separate the western area of diffuse mantle-source CO_2 release, from the eastern area where CO_2 output is lacking as shown in Chiodini et al. (2020). The boundary between the CO_2 gas release zone to the west and the non-degassing area to the east can also be defined by the alignment of seismicity, which starts at the boundary and becomes clearly clustered to the east, in the axial zone of the chain (blue domain in Figs. 2b and 3a). The presence of deep-source fluids has been also assessed in the southern Apennines by Minissale et al. (2019), who reported gas emissions $^3He/^4He$ values in thermal springs indicative of a mantle origin. Minissale et al. (2019) found $^3He/^4He$ values comparable to those of fluid inclusions trapped within olivine and pyroxenes of the Quaternary volcanic products in the Tyrrhenian side of the Apennines (Martelli et al., 2004; Minissale, 2004; Chiodini et al., 2011). Gas emissions and fluid inclusions are signatures of a metasomatized mantle contaminated by subduction-derived fluids with minor contribution of shallow crustal sources (Frezzotti et al., 2009). This is consistent with the deep structure and dynamics of the Apennines region, where westward subduction of the carbonate-rich Adriatic plate occurs beneath the Tyrrhenian lithosphere leading to the formation of carbonatite melts. These fluids are rich in

deeply-derived CO_2 and rise to the surface defining the large Tuscan-Roman (TRDS) and the Campanian (CDS) degassing structures that are both located on the Tyrrhenian flank of the Apennines (Fig. 1c, Chiodini et al., 2004; Frezzotti et al., 2009).

The Apennines have been the locus of numerous destructive historical earthquakes (Fig. 2a), especially in the southern portion of the chain where the strongest shocks have occurred. Studies of the most recent seismic sequences have related the fluid involvement to the earthquake occurrence as well as to the observation of seismic transients (Miller et al., 2004; Di Luccio et al., 2010; Lucente et al., 2010; Terakawa et al., 2010; Chiodini et al., 2011; Malagnini et al., 2012; Calderoni et al., 2015; Chiarabba et al., 2018; Sebastiani et al., 2019; De Matteis et al., 2021). Therefore, the broad and densely monitored Apennine region is the ideal natural laboratory to study the interaction between fluids and seismicity. In this review paper, we investigate the relationship between seismogenesis, CO_2 degassing and active geodynamic processes in the Apennines by studying the role and nature of fluids involved in these processes. We present new datasets, and we revise data from the literature to provide a comprehensive and detailed picture of the dynamics of the Apennines mountain chain. To this aim we compute new maps of i) the seismogenic thickness using the instrumented seismicity from the Italian seismic network, and ii) the geodetic velocities and strains, computed from the continuous GNSS networks. We compare these datasets to the earthquake moment tensors distribution, the CO_2 release, the Moho depth, seismic velocities, active faults, heat flow and Bouguer gravity anomalies.

2. Geodynamic setting of the Apennines and origin of carbon dioxide

The Tyrrhenian-Apennines-Adriatic system is located in the central Mediterranean and is composed of the Apennines fold-and-thrust belt, the Tyrrhenian back-arc basin, the Calabrian Arc and the Adriatic-Ionian foreland (Fig. 1). The Apennines are part of the central Mediterranean orogenic belt and originated from the convergence between the African and Eurasian plates during the Late Cretaceous-Quaternary (Malinverno and Ryan, 1986). This fold-and-thrust belt developed mainly in Neogene times through the subduction and roll-back of the Adriatic-Ionian lithosphere in

the larger framework of slow Eurasian-African convergence (Dewey et al., 1989; Patacca et al., 1990; Doglioni, 1991; Faccenna et al., 2001). The northern and southern Apennines form major arcs that include the Adriatic and Ionian foreland, respectively (Fig. 1c), whose geometry mainly reflects the Mesozoic paleogeographic complexity, the subducting plates configuration and the subduction evolution (Gattaceca and Speranza, 2002; Faccenna et al., 2014). The central Apennines (Fig. 1c), between the northern and southern segments of the orogenic belt, is characterized by a complex deformation pattern with folds and thrusts, some with high angles such as in the Gran Sasso area (Speranza, 2003; Satolli et al., 2005).

The formation of the northern Apennines orogenic belt initiated in the Late Cretaceous due to the subduction of the Piedmont-Ligurian oceanic basin under the Eurasian plate that produced the Ligurian accretionary complex (Carmignani et al., 1994; Marroni et al., 2010 and references therein). The oceanic subduction continued up to Early Eocene, when the Adriatic continental lithosphere approached the trench (Rosenbaum and Lister, 2004; Molli, 2008). The subsequent evolution of the Apennines orogenic belt occurred in the context of the continental collision between the Eurasian plate and Adria microplate, and the west-dipping subduction of the Adriatic continental lithosphere. The front of the advancing Ligurian accretionary prism was overthrusted onto the Meso-Cenozoic sedimentary successions of the passive margin of Adria, which were in turn progressively deformed to produce the northern Apennines thrust belt (Marroni et al., 2010). The Oligocene-Neogene tectonic evolution was characterized by the eastward migration of the thrust belt - foredeep basin system towards the Adriatic foreland (Patacca et al., 1990).

In the southern Apennines, the orogenic belt is made up of three elements that reveal the complexity of the convergence processes (Patacca and Scandone, 1989; Catalano et al., 2004). These consist of thrust sheets that incorporate Meso-Cenozoic units belonging to the African and Eurasian continental paleomargins (Adriatic plate and Corsica Sardinia block) and to the Neotethys oceanic basin: i) the uppermost structural element includes the Calabride crystalline nappe (Eurasian paleomargin), ii) the intermediate element is formed by the Sicilide and Ligurian nappes

(Neotethyian domain) interpreted as remnants of the Oligocene-Miocene accretionary prism developed during oceanic subduction, iii) the lowermost element, representing the backbone of the Apennines, is formed by basinal and carbonate platform sequences of the Adria paleomargin domains that were incorporated in the accretionary prism in Late Tortonian - Early Pleistocene times (Catalano et al., 2004). This post-Tortonian phase corresponds to a major change in the tectonic evolution of the southern Apennines characterized by the spreading of the southern sector of the Tyrrhenian back-arc basin (Patacca and Scandone, 1989). Extension in the Tyrrhenian basin and thrusting in the mountain belt coexisted and migrated rapidly eastward in response to the passive retreat of the subducting Adriatic-Ionian lithosphere. The southern Apennines and the Calabrian arc connect with each other beneath the Pollino ridge (Fig. 1c), which is floored by thick thrust-imbricated SW-dipping inverted carbonate sequences of Mesozoic-Tertiary age overthrusted by Ligurian carbonates (Filice and Seeber, 2019).

The Adriatic continental and Ionian oceanic lithospheres are considered a rigid promontory of Africa since at least Jurassic time (Channell et al., 1979; Rosenbaum et al., 2004). However, paleomagnetic studies indicate that Adria may have rotated counterclockwise by as much as 20° relative to Africa since ~20 Ma (Márton, 2003; Márton et al., 2008, van Hinsbergen et al., 2014). Also, the formation of NW-SE trending rifts along the African margin in the Sicily Channel (Fig. 1a) during the Miocene would support the relative motion of Adria away from Africa in the Neogene (Civile et al., 2010). Independent motion and fragmentation of Adria is also suggested by the present-day GNSS velocities (e.g., D'Agostino et al., 2008) and the lithospheric seismic velocity structure across the Adriatic recently imaged in 3D full waveform tomography (Magnoni et al., 2022).

Since Middle Miocene, extension along the Tyrrhenian margin resulted in crustal thinning of the internal sectors of the orogenic belt (Casero et al., 1988; Patacca et al., 1990; Cello and Mazzoli, 1999). The spreading of the Tyrrhenian basin occurred in two distinct episodes (Marani and Trua, 2002; Nicolosi et al., 2006), the earlier opening stage which occurred from ~12-9 Ma to

6-5 Ma and was characterized by widespread extension in the northern domain and rifting in the western part of the southern domain, and the later, faster episode of opening (50-80 mm yr^{-1}; Faccenna et al., 2001) in the southern domain that led to the formation of the Vavilov (5-4 Ma; Fig. 1b) and Marsili (3-2 Ma; Fig. 1b) oceanic basins (Rosenbaum and Lister, 2004).

Extension related to the opening of the Tyrrhenian Sea progressed from west to east forming coastal and intermountain basins. Along the chain axis, Late Pliocene - Quaternary continental basins developed in the hanging-wall of NW-SE striking high-angle normal faults, which crosscut the preexisting contractional structures (Hyppolite et al., 1994; Galadini, 1999; Ghisetti and Vezzani, 2002; Piccardi et al., 2006). Contractional deformation is ongoing in the northern Apennines along the outermost thrust systems of the Emilia, Ferrara and Adriatic arcs (Bonini et al., 2014 and references therein). Thrusting at the front of the southern Apennines (Patacca and Scandone, 2001) ceased in the Lower Pleistocene, and the axial belt was in turn affected by NE-SW regional extension since the Middle Pleistocene (Hyppolite et al., 1994). The subduction and south-eastward roll-back of the Ionian slab beneath the Calabrian Arc, slowed down since the Middle Pleistocene, likely due to an overall rearrangement of the south-central Mediterranean tectonics (Goes et al., 2004). Evidence of present-day remnants of the former extensive subduction activity are the subcrustal earthquakes occurring down to 90 km depth below the northern Apennines (Selvaggi and Amato, 1992) and the deep earthquakes concentrating offshore western Calabria, depicting a ~200 km wide and a sub-vertical elongated slab (down to 500 km depth) sinking below the southern Tyrrhenian basin (Selvaggi and Chiarabba, 1995). However, no subcrustal seismicity is recorded in the southern Apennines (Chiarabba et al., 2005). The stretched crust along the Tyrrhenian margin was affected by widespread Plio-Quaternary volcanism extending from the Tuscan Province (TRDS) to the Campanian volcanic zone (Vesuvius, Phlegrean Fields and Ischia), where magmatism is still active. To the south, volcanism concentrates in the Aeolian volcanic arc and in eastern Sicily (Etna volcano). Rocks of these magmatic provinces are commonly considered “orogenic” or “subduction-related”, to indicate a

generation from mantle sources modified by the addition of fluids or melts from the subducting lithosphere (Peccerillo and Lustrino, 2005). Two exceptions are Mount Etna and Mount Vulture volcanoes. Mount Etna has a very weak contribution from subduction-related components being geochemically and isotopically akin to ocean-island basalts. Mount Vulture, an isolated volcano at the border of the Apulia foreland and east of the Apennines compressive front, shows peculiar intermediate compositions of subduction-related metasomatism and enrichment of "anorogenic" components, that did not undergo compositional modification by young subduction processes (Beccaluva et al., 2002; Peccerillo and Lustrino, 2005).

The Apennines fold-and-thrust belt includes Mesozoic to Neogene sedimentary successions representative of different paleogeographic domains (i.e., Eurasian, Adriatic, and Neotethys domains), and of the Miocene-Pliocene foredeeps. The northern Apennines includes Triassic-Miocene sedimentary successions (basal clastics deposits, evaporites, shallow-to-deep water carbonates and basinal pelagic units) deposited along the margin of the Adria plate (Fantoni and Franciosi, 2010), which were overthrusted during the Oligocene-Early Miocene by the Ligurian complex, i.e. an accretionary complex of deep-marine sediments and mafic rocks derived from oceanic crust (Vitale et al., 2013). In the Tuscany region, the orogenic belt consists of three structural elements: i) the uppermost ocean-derived Ligurian unit that overthrusts the units below ii) the non-metamorphic Tuscan Nappe, which includes sedimentary sequences of the Adriatic passive margin (from Triassic-Jurassic carbonate platform and pelagic limestone, Cretaceous to Early Oligocene carbonate resediments and marls, Oligocene to Lower Miocene foredeep flysch deposits), iii) the lowermost structural element is the Hercynian basement that was metamorphosed at HP/LT conditions at ~25 Ma (i.e., Tuscan Metamorphic Complex; Carmignani and Kligfield 1990). The deformation phase that produced the tectonic nappe stack occurred between the Late Oligocene and Early Miocene.

The northern portion of the central Apennines includes sedimentary sequences of the Umbria-Marche and Laga domains mainly consisting of i) Late Triassic-Early Jurassic platform

carbonates and evaporites, ii) Jurassic - Oligocene basinal deposits (pelagic limestones, resedimented carbonates, marls), iii) Miocene basinal-to-foreland terrigenous and marly deposits, and iv) Messinian flysch of the Laga foredeep domain (Barchi et al., 2003, 2012). To the south, the thrust sheet units of the central Apennines mainly consist of platform-to-slope Mesozoic-Paleogene carbonates (Cosentino et al., 2010; Vezzani et al., 2010; Patacca et al., 2008). The southern Apennines include Meso-Cenozoic sedimentary successions of shelf platform and basin domains of the Adria passive margin, and Mio-Pliocene foredeep siliciclastic successions (i.e., the Campania-Lucania platform and the Lagonegro Basin units; Patacca and Scandone, 2007). These units, detached from the basement, overthrusted the Apulian carbonate platform that was in turn embodied in the thrust-fold belt in Late Pliocene-Early Pleistocene times (Patacca and Scandone, 2001). While the stack of rootless units is interpreted in terms of thin-skinned tectonics, the structural architecture of the buried Apulian thrust sheets indicates that the final shortening phase was governed by thick-skinned tectonics (Butler et al., 2004; Mazzoli et al., 2008).

Outcropping faults are characterized by Late Pleistocene-Holocene and Quaternary slip-rates in the 0.1-1.5 mm yr^{-1} range with higher values mainly associated with the normal faults dissecting the axial mountain belt (Galadini and Galli, 2000; Ferranti et al., 2014 and references therein). Active, WNW-ESE to NW-SE-oriented thrust-and-fold systems define the eastern outer front of the northern Apennines buried beneath the Po plain and the Marche Plio-Quaternary foredeep (Fantoni and Franciosi, 2010). Conversely, the Apulian foreland is characterized by active, W-E striking shear-zones that extend westward underneath the outer Apennines belt (Di Bucci et al., 2010).

The origin of the widespread CO_2 Earth degassing processes (~2.1×10^{11} mol yr^{-1}) recognized on the Tyrrhenian side of the Apennines and in some major extensional seismogenic zones of the chain axis (Chiodini et al., 2004), is suggested to be related to the crustal carbonates lithologies of the subducted Adriatic microplate that are trapped in the mantle wedge at depth and melt due to the elevated isotherms in the back-arc region (Frezzotti et al., 2009). Partial melting of

these lithologies produces carbonate-rich melts that are upwelling at about 60-70 km depth, which in turn metasomatize the mantle wedge and favor a continuous CO_2-flux from the mantle to the crust. These CO_2-rich fluids may undergo contamination while ascending to the surface and passing through the local lithologies including the carbonate thrust-sheets of the Apennines (Italiano et al., 2000; Ascione et al., 2018). On the Tyrrhenian side of the Apennines, the diffuse release of deeply derived CO_2 at the surface is favored by the enhanced vertical permeability of the stretched crust related to Pleistocene-Holocene normal faulting (Ghisetti and Vezzani, 2002), but abruptly disappears close to the Apennines seismic belt where instead the formation of highly pressurized structural traps in the crust is favored, as also observed in deep oil wells (Chiodini et al., 2010; Improta et al., 2014).

3. Seismotectonic picture of the Apennines

In the continental subduction/collision domain and extensional collapse, the complex interaction among the African and Eurasian plates and the Adria microplate generated most of the destructive earthquakes that occurred along the Apennines. Historical earthquakes are distributed along the chain axis with the maximum magnitude (M^{max}) increasing southward (Fig. 2a; Rovida et al., 2022; https://emidius.mi.ingv.it/CPTI15-DBMI15/query_eq). Over the last seven centuries, frequent historical earthquakes with M^{max}6.5 have occurred across the northern Apennines, while in the central and southern belt the reported maximum magnitude is 7.1 (Fig. 2a), with most of the largest events concentrated in the southern Apennines.

The INGV national seismic network (Fig. 1b), which developed after the occurrence of the 1980 M_S 6.9 Irpinia earthquake (Cocco and Pacor, 1993), is presently comprised of about 500 stations that allow for an accurate representation of the instrumented seismicity over the Italian peninsula (Italian Seismological Instrumental and Parametric Database, ISIDe Working Group, 2007). The ISIDe Database (Fig. 2b) shows two main arc-shaped belts, roughly following the chain axis that are consistent with the historical events distribution. While the northern arc is characterized by a continuous (and narrow) seismicity distribution without significant gaps, the

southern arc has events arranged in clusters (Fig. 2b) as in the Pollino Massif where low to moderate magnitude earthquakes (M^{max}5.5) occur (e.g., Totaro et al., 2014). After the 1980 Irpinia earthquake other large seismic events struck the Apennines belt, such as those of the 1997-1998 Umbria-Marche sequence (M_w^{max}6.3, Miller et al., 2004), the 2009 L'Aquila earthquake (M_w6.3, Di Luccio et al., 2010), the 2012 Emilia seismic sequence (M_w^{max}5.9, Govoni et al., 2014) and the 2016-2017 Amatrice-Norcia seismic sequence (M_w^{max}6.5, Chiarabba et al., 2018; Gunatilake and Miller, 2022).

Seismicity is usually shallow with focal depths of 10-15 km and concentrated within a ~50 km wide belt (Fig. 2b) along the Apennines (Chiarabba et al., 2005, 2016). Moment tensor solutions of M_w>4 earthquakes (Fig. 2c) reveal tension axes generally orthogonal to the trend of the mountain belt (Pondrelli et al., 2006; Herrmann et al., 2011, Scognamiglio et al., 2016). The active faults of the Apennines have a prevailing NW-SE strike (Fig. 1c) and overlap with the seismic belt. Slip on these faults is characterized by a normal faulting stress regime with NE-SW extension (Mariucci and Montone, 2020). In contrast, the Apulian foreland is characterized by the occurrence of sparse moderate-magnitude earthquakes with hypocentral depths down to 35 km (Chiarabba et al., 2005; Di Luccio et al., 2005a, 2005b; Ventura et al., 2007). In the Apulian foreland, seismicity is distributed along an E-W belt with events showing strike-slip and reverse focal solutions in the Gargano region (Fig. 2c), while reverse moment tensor solutions (Fig. 2d) characterize the northern Adriatic foreland (Scognamiglio et al., 2016) defining a dominant NE-SW compression (Mariucci and Montone, 2020). On the Tyrrhenian side, seismicity is arranged in patch-like clusters (Fig. 2b) that are mainly located in the volcanic and geothermal areas (Larderello in Tuscany; Albani Hills, Latium; the Campanian Vesuvius and Phlegrean Fields volcanoes, Fig. 1c for locations). In these areas, focal mechanisms are highly heterogeneous, reflecting the complex spatial and temporal variations of the local stress field (Frepoli et al., 2010; D'Auria et al., 2014).

Low frequency seismic events and transient signals recorded in the northern and central Apennines (Piccinini and Saccorotti, 2008; Calderoni et al., 2015) have provided evidence for the

presence of fluids in the crust where fractured seismogenic volumes exist. Numerous studies have evaluated the primary role that CO_2-rich fluids play in the Apennines seismogenic process of upper crustal normal faulting earthquakes. The presence of high-pressure CO_2 at depth explains the aftershocks spatio-temporal pattern of the 1997 Umbria-Marche sequence in the northern Apennines (Miller et al., 2004). Twelve years later, the central Apennines were hit by the 6 April 2009 M_w6.3 L'Aquila earthquake, for which seismological (Di Luccio et al., 2010; Lucente et al., 2010; Terakawa et al., 2010; Malagnini et al., 2012) and geochemical analyses (Chiodini et al., 2011) have shown an initial phase of increased pore fluid pressure until the occurrence of the mainshock when pore pressure diffusion occurs through the upward migration of fluids, in agreement with the evolution of the sequence. Ventura and Di Giovambattista (2013) and Pezzo et al. (2018) invoked a pore pressure increase that reactivated buried thrust faults in the northern Apennines where the 2012 M_w5.8 Emilia earthquake occurred. Napolitano et al. (2020) and De Matteis et al. (2021) have provided seismological evidence that the 2010-2014 Pollino swarm-like seismic sequence in the southern Apennines (M_L^{max}5.0) was driven by a fluid-filled crack in the seismogenic volume. Combining seismological and geochemical analyses, Di Luccio et al. (2018) proved that the fluid pressure redistribution in the crust of the southern Apennines caused the 2013-2014 Sannio-Matese sequence. Additionally, a recent comparison of the 10-year (2009-2018) record of tectonic CO_2 emissions and seismicity in the central Apennines, provided evidence that high-pressure gas pockets at depth may have weakened the nearby fault system causing earthquakes (Chiodini et al., 2020). Chiarabba et al. (2018) also demonstrated that the M_w6.0 Amatrice and the M_w6.5 Norcia earthquakes that struck central Italy in 2016 occurred on distinct faults overlying an overpressurized volume. In the southern Apennines, the presence of CO_2-pressurized gas reservoirs in the seismogenic volume of the 1980, M_S6.9 Irpinia earthquake has been documented in local earthquake tomographic images and deep boreholes (Improta et al., 2014; Amoruso et al., 2014). The above studies highlight the role of fluids in the earthquake triggering mechanism and in modulating the space-time evolution of the sequences through diffusive processes. Two notable

exceptions are the 1990-91 M_w^{max} 5.7 Potenza (Di Luccio et al., 2005b) and the 2002 M_w5.8 Molise (Pino and Di Luccio, 2005a; Di Luccio et al., 2005a; Vallée and Di Luccio, 2005) seismic sequences that occurred along deep, blind strike-slip structures in the external zone of the Apennines.

4. Geochemical dataset and fluid release

In the last decades, in the Apennines fold-and-thrust belt the link between fluids, mainly CO_2, and seismicity has been widely recognized with the CO_2 rich reservoirs stored in the seismogenic volumes of the crust (Chiodini et al., 2004; Miller et al., 2004; Di Luccio et al., 2010; Lucente et al., 2010; Terakawa et al., 2010; Chiodini et al., 2011; Malagnini et al., 2012; Ciotoli et al., 2014; Calderoni et al., 2015; Amoroso et al., 2017; Chiarabba et al., 2018; Sebastiani et al., 2019; De Matteis et al., 2021; De Landro et al., 2022; Cultrilake and Miller, 2022). Moreover, the major seismic sequences were accompanied by an increase in the gas emissions within the major aquifers (Chiodini et al., 2020). Using methods and data from earlier investigations, we report in Fig. 3a the amount of deeply-derived CO_2 injected into the major aquifers of the region (Chiodini et al., 2000, 2004). The Apennines mountain chain separates the eastern non-degassing area from the Tyrrhenian region where diffuse deeply-derived CO_2-rich fluids define the TRDS to the north and the CDS to the south (Fig. 3a) (Frezzotti et al., 2009). In the TRDS, the CO_2 flux is diffuse with larger values in the Tuscany geothermal fields and the Albani Hills (central Latium, Fig. 1c for location) The CDS is, however, characterized by values of CO_2 flux well above 1 t $d^{-1}km^{-2}$. Approaching the chain axis, CO_2 is likely stored in crustal reservoirs and rises to the surface through the highly fractured zones of the Apennines, where it is dissolved in the large aquifers (Chiodini et al., 2004, 2020).

The $^3He/^4He$ ratio is a measure of the changes in the balance between the typically crustal (^4He) and mantle-derived (^3He) components of the total volatile inventory and is therefore also a powerful indicator of mantle degassing (Lupton, 1983; Minissale et al., 2019 and references therein). In geochemical studies, $R=^3He/^4He$ represents the sample corrected for atmospheric

contributions, and R_a is the $^3He/^4He$ ratio of air, thus often R/R_a is used instead of $^3He/^4He$. In the southern Apennines, the area north of the Pollino region has R/R_a values in the 0.1-0.2 range suggesting a nearly null mantle source contribution (Apollaro et al., 2020). On the other hand, by combining data from new sites with previous work (Italiano et al., 2000; Minissale, 2004; Caracausi et al., 2013), Ascione et al. (2018) have shown that the Sannio-Matese region is characterized by R/R_a between 1.4 and 2.8. Values of R/R_a between 2.4 and 2.8 also are found at the Mefite D'Ansanto site, a large region of natural low-temperature CO_2-rich gas emission in a non-volcanic environment in the Irpinia region (Italiano et al., 2000; Chiodini et al., 2010). These values are close to those measured in fluid emissions and melt inclusions at the Vesuvius and Phlegrean Fields volcanoes, which show R/R_a in the range of 2-3.2 (Italiano et al., 2000; Martelli et al., 2004). In the central Apennines, fluid inclusions in the Latium volcanoes have R/R_a values between 0.4 and 1.7 (Martelli et al., 2004). The Velino aquifer in the Abruzzi region has very low R/R_a values (<0.2, Chiodini et al., 2011) that are comparable to those found in the Pollino mountain range. These low values were ascribed to the long residence time of gases in overpressurized crustal reservoirs at the bottom of the seismogenic layer thus increasing their radiogenic ^4He (Chiodini et al., 2011). Therefore, based on the above observations, excluding the preeminent crustal component in the Pollino area and in the Velino aquifer and considering the He isotopic signature of the fluid inclusions in volcanic products, the dominant fluid source in the southern Apennines (Sannio-Matese and Irpinia) is the mantle and the crustal component increases northward.

5. Geophysical observations

In the following we present an overview of the geophysical observations collected in the last decades for the Apennines, including both published datasets (conductive heat flow, Moho depth, Bouguer gravity anomalies, geodetic and seismic strain-rates estimations) and new results obtained in this study (seismogenic thickness and surface deformation).

5.1 Heat flow

The geothermal heat flow of Italy has been investigated since the 1970s through numerous temperature-depth measurements collected in sedimentary basins, shallow sea floor and lake sediments, and shallow and deep geothermal/hydrocarbon exploration wells which allowed for the compilation of numerous maps with increasing detail and quality over time (Mongelli et al., 1991; Hurtig et al., 1991; Cataldi et al., 1995; Della Vedova et al., 2001). In this study (Fig. 3b) we refer to the compilation reported in Della Vedova et al. (2001), where the first discrimination of the contributions from shallow processes (such as water circulation, recent fast sedimentation, and magmatic activity) that strongly affect the surface heat flow, was attempted. A broad anomalous area with high heat flow values, larger than 100 mW m^{-2} (up to 400 mW m^{-2}), can be observed over Tuscany and Latium (Fig. 3b), which is related to the high enthalpy geothermal systems of the Pliocene-Quaternary volcanic areas and/or intrusions (Peccerillo and Lustrino, 2005). Three other small areas characterized by moderate-to-high heat flow values can be recognized in the map (Fig. 3b). The first area corresponds to the Mefite D'Ansanto degassing site (Chiodini et al., 2010). The second one is related to the active Phlegraean Fields - Vesuvius volcanic complex, while the third one (Filippucci et al., 2019) corresponds to a crustal thermal source beneath the Candelaro fault, just south of the Gargano Promontory (Fig. 1c for location).

Furthermore, a large belt, containing the southern Apennines mountain ridge and the westernmost Apulian foreland (Fig. 3b), is characterized by heat flow values of ~50-100 mW m^{-2}. Heat flow values are generally low (20-40 mW m^{-2}) in a large zone including most of the central Apennines and the Tyrrhenian flank of the southern Apennines, where significant infiltration and circulation of meteoric waters within the carbonate aquifers occur. Moreover, as observed by Chiodini et al. (2021), the advective heat flow values measured in the Apennines carbonatic aquifers are comparable to the larger conductive heat flow estimates measured in the geothermal and volcanic areas of the Tyrrhenian side of the Italian peninsula.

5.2 Moho depth

Numerous studies have focused on determining the Moho topography beneath the Italian region by using different techniques and analyzing data acquired by active and passive source seismic experiments. In the last thirty years, the INGV national broadband seismic network has continuously expanded over the Italian territory allowing for the acquisition of large volumes of high-quality seismic records (Fig. 1b). Parts of this seismic database has been analyzed by many authors applying different techniques such as local earthquake tomography, receiver functions and ambient noise tomography to provide an improved map of the Moho depth (Piana Agostinetti et al., 2009; Di Stefano et al., 2009, 2011; Molinari and Morelli, 2011; Verbeke et al., 2012; Spada et al., 2013; Manu-Marfo et al., 2019; Chiarabba et al., 2020 and references therein) and the main features of the Moho topography are quite similar among these different studies.

In our paper we refer to the study of Spada et al. (2013) where the Moho depth was obtained by the integrated analysis of controlled-source seismology and receiver functions (Fig. 3c). In the western Apennines, the Moho exhibits a significant depth variability with values ranging from 20 to 50 km (Fig. 3c). In the Adriatic foreland, the Moho depth spans in the range 32-38 km and deepens to 50 km depth as it approaches the axial zone of the Apennines to the west. Beneath the chain axis the Adriatic Moho is overlaid by the shallower (~30-32 km) Tyrrhenian Moho and the vertical separation between the two Mohos defines a step of ~25 km underneath the northern and the southern Apennines and of ~10 km beneath the central Apennines (Fig. 3c). The Tyrrhenian Moho becomes shallower (20 km) moving towards the back-arc region to the west.

5.3 Bouguer Gravity Anomalies

The most recent gravimetric map of Italy was compiled by the Italian Agency for Environmental Protection and Technical Services (APAT, now ISPRA) from land and sea data collected over the previous 40 years by ENI S.p.A., OGS and ISPRA (Ferri et al., 2005). The regional gravity map (Fig. 3d) is characterized by relative gravity lows running parallel to the axial zone of the mountain belt, surrounded by areas of gravity highs. In the southern Apennines the

negative Bouguer anomalies define a narrow strip with values up to -100 mGal in the foreland except in the southeastern part of the region where carbonates outcrop (Puglia region). Towards the north, negative values characterize a wider region encompassing the central and northern Apennines including the western Adriatic region (Fig. 3d). Positive Bouguer anomalies are observed along the Tyrrhenian margin of Italy (up to 100 mGal).

At the local scale, the Bouguer anomalies correlate well with the surface geological features, highlighting their contribution to the local subsurface gravity effects. This can be readily observed along the Marche and Abruzzo coastal areas and the Po valley where the local negative gravity anomalies coincide with the spatial distribution of the thicker foredeep deposits (~5000 m, Bally et al., 1986). Bouguer anomalies with wavelengths larger than 80 km (Fig. 3d) are related to deep sources, as for instance the Moho topography (Fig. 3c) (Cassinis et al., 2003).

5.4 Seismogenic thickness

We provide a comprehensive map of the seismogenic thickness variations across the Apennines, by discretizing the region into 0.4°x0.4° cells with a 75% spatial overlap and computing the depth distribution of the epicenters that fall within each cell. We use as input the INGV earthquake catalog (ISIDe Working Group, 2007) that includes events from 2005 to April 2021 with magnitudes larger than 1.5 to avoid possible biases on the seismogenic thickness estimation due to the smaller magnitude events usually located at shallow depth. Following Smith-Konter et al. (2011), for each cell containing at least 35 events we defined the seismogenic thickness as the depth of the 90^{th} percentile of the hypocentral depth distribution within that cell. Results (Fig. 4a) show that beneath the northern and central Apennines the seismogenic layer follows the curvature of the chain axis and reaches values down to 30 km and below in the foreland, while it shows values in the range of 10-15 km in the Tyrrhenian domain. Southward, the seismogenic thickness thins westward beneath the Tyrrhenian coast and thickens approaching the Calabrian Arc (to the south) and the Apulian foreland (to the east). The thickening of the

seismogenic layer occurs in a very narrow belt (~30 km wide) beneath the northern and central Apennines, while it occurs over a wider region (~50-70 km) beneath the southern Apennines.

5.5 Surface deformation

The first GNSS measurements along the Apennines date back to 1991 with the monitoring of a temporary regional network of 35 benchmarks (Anzidei et al., 2001). In the same year, the continuous GNSS station of MATE (close to the city of Matera) operated by ASI (http://geodaf.mt.asi.it) was also installed. Since then, several local and regional temporary (Ferranti et al., 2008; Giuliani et al., 2009; Bennett et al., 2012; Galvani et al., 2012; Cambiotti et al., 2020; Carafa et al., 2020; Esposito et al., 2020) and permanent networks, operated by local institutions, agencies, universities and research institutes (Devoti et al., 2017 and references therein for details), have been extensively deployed for crustal deformation studies and commercial applications (mapping and engineering applications) along the whole Italian territory. Therefore, in the last two decades, many GNSS episodic benchmarks have been resurveyed, new studies including new continuous GNSS sites have been published (D'Agostino et al., 2009; Serpelloni et al., 2013; Métois et al., 2015; Devoti et al., 2017, Chiarabba and Palano, 2017), and velocity uncertainties have been reduced. These studies found a sharp divergence of the horizontal velocity field along the topographic relief of the Apennines chain, which is characterized by a prevailing NNE motion of ~4-6 mm yr^{-1} along the Adriatic side and with ~1-3 mm yr^{-1} NNW motion along the Tyrrhenian side, in a Eurasian reference frame. Regarding the vertical motion, very few solutions are currently available and define a general uplift of the Apennines belt (Serpelloni et al., 2013; Faccenna et al., 2014; Devoti et al., 2017).

To provide an updated image of the deformation pattern of the Apennines, we analyzed an extensive dataset consisting of ~900 continuous GNSS stations with more than 2.5 years of observations. Raw GNSS observations were processed using the GAMIT/GLOBK software packages (Herring et al., 2018) and adopting the strategy described in Palano et al. (2020). The resulting velocity field is shown in Fig. 4b where a Eurasian reference frame is assumed.

We also estimated the horizontal strain-rates (Fig. 4c) over the investigated area using the method of Shen et al. (2015), computing the horizontal velocity gradients on regularly spaced grid points (0.25°x0.25°) by least squares inversion of the observed GNSS velocities. The method considers optimal weighting functions of the data, allowing a finer resolution, especially in regions characterized by sparsely distributed data.

Our new horizontal velocity field (Fig. 4c) confirms, with a higher spatial resolution, both the sharp divergence along the Apennines chain axis and the general pattern of motion identified in previous studies. Regarding the vertical deformation pattern (Fig. 4b), most of southern Apennines and the Apulian foreland are characterized by a general uplift of ~1 mm yr^{-1}. Uplift of ~1 mm yr^{-1} can be also observed in the volcanic and geothermal areas (Larderello, Albani Hills, Vesuvius and Phlegrean Fields; see Fig. 1c for locations), while all the stations located along the Adriatic foreland are currently subsiding with rates in the 0.5 - 2 mm yr^{-1} range. The strain-rate field (Fig. 4c) depicts a near continuous belt of high values with prevailing NE-SW principal extensional axes along the Apennine chain. The strain axis shows trends that are roughly orthogonal to the chain belt in the northern sector, while in the southern one the strain directions are more heterogeneous. The northern Apennines are further characterized by extension rates between 25 and 50 nanostrain yr^{-1} in a relatively wide area (~50 km), that becomes wider (~100 km) across the central Apennines with similar extension rates (35-50 nanostrain yr^{-1}). In the southern Apennines, the strain-rate field is characterized by values up to 45 nanostrain yr^{-1} mainly confined to the CDS zone (see Fig. 1c for locations). Outside the chain axis, maximum dilatation values occur locally in the Campanian volcanic area and north of the Gargano promontory (Fig. 4c). Contraction of ~20 nanostrain yr^{-1} with a prevailing N-S-oriented axis is observed along the Po valley. The Apulian foreland is also characterized by a small contraction (5-10 nanostrain yr^{-1} with variable orientations), which becomes more marked (up to ~30 nanostrain yr^{-1} with NW-SE-oriented axis) in the Gargano promontory. Another local patch of contraction is observed in the Tyrrhenian offshore region, northwest of the Phlegrean Fields (Fig. 4c).

5.6 Geodetic and seismic strain-rates

To date, few studies have compared geodetic and seismic deformation budgets to shed light on the seismic hazard of the Apennine chain. Earlier Ward (1988) estimated a seismic-to-geodetic deformation ratio of about 71% between seismic and Very Long Baseline Interferometry (VLBI) strain-rates, averaged over the whole Italian peninsula. Pondrelli (1999), using regional moment tensors, found that seismicity accounts for only about 30% of the total deformation along the Apennines, inferred from VLBI data. Using triangulation measurements and instrumented seismicity spanning a period of 126 years, relevant discrepancies have been also documented along the Apennines by Hunstad et al. (2003), who found a decoupling ratio in the range of 7-68%. In the southern Apennines Jenny et al. (2006) observed that the seismic deformation budget is compatible with the full tectonic one. These previous studies were significantly hampered by the sparse distribution of geodetic data, while recent works by Palano et al. (2011) and D'Agostino (2014) provided a much more detailed geodetic strain-rate field therefore leading to an improved estimation of the seismic and geodetic deformation budgets. Palano et al. (2011) compared the geodetic strain-rates with those derived from a 600-year seismicity catalog over a 0.2°x0.2° grid sampling the southern Apennines region. They observed a good agreement between the seismic and geodetic strain-rates along the southern Apennines crest, and a significant discrepancy (ratio less than 20%) on the Matese Mountains, and between Irpinia and Pollino. The authors highlighted that the observed discrepancy might suggest an increased probability of future earthquakes. Comparing the geodetic strain-rates with those from the seismicity released in the last ~500 years along the entire Apennines chain, D'Agostino (2014) found that these contributions agree within the uncertainties, and that the deformation budget yields an average recurrence interval of 30-75 years for $M_W \geq 6.5$ events.

The increasing number of continuous GNSS stations coupled with the availability of numerous episodic benchmarks with long time-series span, have recently permitted the possibility of comparing the geodetic and the geologic strain-rates at the scale of regional fault systems.

Studies focusing on this topic have provided new insights on the partitioning between fault slip and bulk lithosphere permanent strain (Ferranti et al., 2014; Carafa et al., 2017, 2020). Ferranti et al. (2014) compared geodetic and geologic moment-rates for 32 active faults cutting the Southern Apennines and observed that the geodetic rates are largely at the upper bound of the geological rates. Similar results have been presented by Carafa et al. (2017 and 2020), which relate the observed excess of geodetic strain-rate to additional processes like upper crustal viscoplastic deformation and aseismic slip or indicate missing faults in the adopted database. Despite the overall good agreement between the geodetic, geologic, and seismic deformation-rates for the Apennines chain, a few local discrepancies along the southern Apennines suggests that in this region a percentage of the deformation budget cannot be entirely associated with elastic tectonic processes.

5.7 The seismic structure

Seismic tomography studies of the crust and mantle beneath the Italian peninsula have been based on a variety of data types and approaches, producing several three-dimensional seismic velocity models at different scales and resolution. These studies are mainly based on either travel time tomography of earthquakes at regional and/or teleseismic distances (Lucente et al., 1999; Wortel and Spakman, 2000; Piromallo and Morelli, 2003; Giacomuzzi et al., 2011, 2012; Di Stefano and Ciaccio, 2014), or the inversion of surface wave dispersion curves from earthquakes and/or ambient noise (Molinari et al., 2015; Manu-Marfo et al., 2019). Beneath Italy, at upper mantle depths, the main common features to all tomographic models are the high seismic velocity anomaly of the Calabrian-Apenninic slab interpreted as cold subducted lithosphere, and the low wave speed anomaly of the Tyrrhenian back-arc region interpreted as asthenospheric material (Lucente et al., 1999; Wortel and Spakman, 2000; Piromallo and Morelli 2003; Giacomuzzi et al., 2011, 2012; Molinari et al., 2015; Manu-Marfo et al., 2019). A discontinuous distribution of high velocity anomalies below the orogenic belt has been related to possible lithospheric detachments and/or tears in the topmost mantle (Wortel and Spakman, 2000). Beneath the northern and central Apennines, the mid-lower crust is characterized by a continuous low seismic velocity (Vp and Vs)

zone that follows the belt axis and is interpreted as subducting crustal material (e.g., Giacomuzzi et al., 2011, 2012). In turn, the upper crust shows short-wavelength seismic velocity variations that define high- and low-velocity patterns corresponding to platform carbonates and basinal units, respectively (Di Stefano et al., 2009; Calò et al., 2012; Viganò et al., 2013; Di Stefano and Ciaccio, 2014; Amoroso et al., 2014; Totaro et al., 2014; Molinari et al., 2015; Improta et al., 2014; Improta et al., 2017; Bagagli et al., 2020; Napolitano et al., 2020; De Matteis et al., 2021; De Landro et al., 2022).

To investigate the link between the seismic structure and fluids beneath the Apennines, we analyze two velocity models representative of the study region and derived by inversion of body-waves travel times, which illuminate the shallow and deep subsurface structure. The first one was obtained from the local earthquake tomography of the crust (Di Stefano and Ciaccio 2014) and the second one from the teleseismic tomography of the upper mantle (Giacomuzzi et al., 2011, 2012). These two models provide Vp, Vs and Vp/Vs ratio and/or their anomalies and are chosen because i) they have a fine resolution at the scale of the entire Apennines, and ii) they invert P and S travel-times at regional (Di Stefano and Ciaccio, 2014) and regional/teleseismic (Giacomuzzi et al., 2011, 2012) distances. To highlight possible correlations with other observables in the study area we prefer to analyze Vs and Vp/Vs anomalies rather than absolute values. Checkerboard tests and the analysis of the model resolution matrix in Giacomuzzi et al. (2012) show that most of the velocity anomalies are well recovered in the Apennine region with 70% resolution of the diagonal elements. In Di Stefano and Ciaccio (2014) synthetic checkerboard tests show high resolution in the shallower layers (above 22 km), while below 38 km depth structural features smaller than 30-45 km are hardly recognizable.

At shallow depths (8 km, Fig. 5a) in Di Stefano and Ciaccio (2014), a nearly continuous belt of negative shear wave velocity anomalies (ΔVs) can be recognized beneath the northern and central Apennines with the largest values in the Adriatic foreland. Negative ΔVs corresponds with the high values of Vp/Vs anomalies (Δ(Vp/Vs)) at the same depth. In contrast, the Tyrrhenian side

of the peninsula exhibits low values of Δ(Vp/Vs) (Fig. 5d). At 22 km depth (Fig. 5b), the central Apennines from the Tyrrhenian to the Adriatic coast show positive ΔVs, whereas the southern Apennines and the eastern border of the northern Apennines are characterized by negative ΔVs. At this depth, the Δ(Vp/Vs) values (Fig. 5e) are relatively low beneath the axial belt, although localized zones of relatively high values are found on the eastern and western side of the chain axis. At 38 km depth (Fig. 5c), the belt of negative ΔVs narrows, even though it is still recognizable especially in the northern Apennines, while positive anomalies are imaged outside the mountain chain, to the east and west. The Δ(Vp/Vs) values (Fig. 5f) are generally low along the Apennines apart from a small area encompassing the boundary between the central and southern Apennines, where high values can be recognized. Below the 38-km depth the resolution of the Vs and Vp/Vs anomaly maps in Di Stefano and Ciaccio (2014) is poor, therefore we refer to the shear wave velocity anomalies from Giacomuzzi et al. (2012) for the upper mantle velocities. The northern Apennines at 60 km depth (Fig. 6a) exhibit strong lateral velocity anomalies from west to east. The positive NW-SE striking ΔVs region elongates below the chain axis and separates two areas of negative velocity anomalies, the south-western one located in Tuscany and the north-eastern one in the Po plain. At the same depth, in the central and partially in the southern Apennines negative ΔVs values extend continuously from the Tyrrhenian to the Adriatic coast, while the southernmost area is characterized by positive velocity anomalies. The Δ(Vp/Vs) maps at 60 km depth show positive values along the Tyrrhenian side, with maxima in the Tuscany and Campania volcanic areas, while the northern and southern Apennines are characterized by negative Δ(Vp/Vs) (Fig. 6d). At 100 km depth (Fig. 6b) positive ΔVs anomalies dominate beneath the Apennines, especially along the chain axis and in the adjacent areas. A strong negative velocity zone is, however, mapped offshore of the Tyrrhenian region extending from the Tuscany coast to the Campanian volcanic area, but in the foreland these low shear wave velocity anomalies are less pronounced. Beneath the Apennines, overall positive Vp/Vs anomalies correlate well with negative ΔVs values at 100 km depth (Fig. 6e). In the northern Apennines a wide region of low Δ(Vp/Vs) extends from west to east reaching

the northern coast of the Adriatic Sea (Fig. 6e). The positive and negative ΔVs anomaly patterns observed at 100 km depth become more evident going deeper into the mantle. In fact, at 160 km depth (Fig. 6c) the ΔVs lows beneath the Tyrrhenian and the northern and southern Adriatic Seas are well localized and separated by ΔVs highs imaged beneath the Apennines. At this depth (Fig. 6f) the observed values of Δ(Vp/Vs) are less prominent than the ΔVs although the overall patterns are comparable. Considering the distribution of the shear wave velocity and the Vp/Vs anomalies at lithospheric depths on the Tyrrhenian side, the Vs lows and the corresponding increase of Δ(Vp/Vs) are possibly related to the upwelling of hot, fluid-rich asthenospheric material.

6. Discussion

The geophysical and geochemical data described in the previous sections are discussed here to highlight their spatial relationship in a comprehensive tectonic and geodynamic picture of the Apennines.

Crustal stretching in the western back-arc region of the Apennines started in the Middle Miocene along the Tyrrhenian side of Tuscany (Barchi, 2010) and in Early Pleistocene times offshore Campania (Milia et al., 2003). Extensional deformation propagated at the western side of the Apennines and the extensional downfaulting superposed onto the Neogene compressional thrust structure migrated progressively from the inner to the axial belt (Hyppolite et al., 1994; Galadini, 1999; Ghisetti and Vezzani, 2002; Piccardi et al., 2006). Conversely, the outer front of the mountain chain and the Adriatic foreland are characterized by active reverse and strike-slip structures, respectively (Louvari et al., 2001; Di Bucci et al., 2009; Viti et al., 2015). Late Pleistocene-Holocene geologic slip-rates estimates are in the 0.1-1.5 mm yr^{-1} interval with the highest values associated with the normal faults dissecting the axial mountain belt (Galadini and Galli, 2000; Ferranti et al., 2014). The marked separation between the eastern and western domains of the Apennines corresponds at depth to the boundary between the westward deepening Adriatic (lower plate) and the overlying Tyrrhenian (upper plate) Moho (Fig. 3c). The overlap region of the Tyrrhenian and Adriatic Moho aligns with the chain axis where a gradient in the Bouguer anomaly

is also observed (Fig. 3d). The Bouguer anomalies with wavelength larger than ~80 km correlate well with the Moho topography suggesting the presence of thinned crust beneath the Tyrrhenian domain and thickened crust beneath the chain axis. The transition between the two domains is also marked by a dense seismicity (Fig. 3b), which is mainly concentrated in a narrow zone along the Apennines chain axis and by a change in the seismogenic thickness estimates (Fig. 4a) from values shallower than 15 km beneath the Tyrrhenian domain and to ~30 km along most of the foreland domain. The prominent increase in seismogenic thickness follows the Moho overlap beneath the axial part of the mountain chain at depth (Fig. 3c) and the near continuous band of extensional geodetic strain-rates (up to 50 nanostrain yr^{-1}; Fig. 4c) at the surface. Focal mechanisms (Fig. 2c) and other shallow stress indicators (Fig. 2d) reveal that the extension affects most of the upper crust beneath the axial region, at least down to the bottom of the seismogenic layer (Fig. 4a).

Significant differences between the western and eastern domains can also be observed at a first glance, in terms of CO_2 degassing (Fig. 3a) and heat flow spatial distributions (Fig. 3b). Most of the western domain is characterized by diffuse mantle-source CO_2 release and high heat flow values (up to 400 mW m^{-2}), especially over Tuscany and Latium. Conversely, the eastern domain is characterized by sparse CO_2 degassing and by lower heat flow values (~50-100 mW m^{-2}). Available shear wave velocity models (Di Stefano and Ciaccio, 2014) at shallow depths along the Apennines highlight the presence of a nearly continuous region of negative ΔVs, which progressively segments and narrows to a strip beneath the northern and southern Apennines down 38 km depth (Fig. 5a, b, c). This pattern of ΔVs anomalies appears poorly correlated with the other observables, especially with the CO_2 degassing and heat flow maps. On the contrary, the pattern of Vp/Vs anomalies (Fig. 5d, e, f) matches with most of the previously described geochemical and geophysical observables especially at shallow depths (~8-22 km).

To summarize the structure of the Apennines at crustal and mantle scales, in Fig. 7, we show the above described observables along a series of SW-NE profiles crossing the different domains of the Italian peninsula with cross-section locations and labels shown in Fig. 7f. The NAP

(Fig. 7a) and CAP (Fig. 7b) profiles cross the northern and central Apennines, respectively. The tectonic complexities of the southern Apennines, however, require a more detailed description of the main features characterizing the lithospheric structure for a better understanding of the role of fluids in the geodynamic setting. To this aim we define three profiles crossing the southern Apennines: the northernmost profile (nSAP, Fig. 7c) runs from the Campanian volcanic area to the Gargano promontory, the central profile (cSAP, Fig. 7d) extends across the Mount Vulture volcano and the southern profile (sSAP, Fig. 7e) intersects the Pollino Massif. In each profile in Fig. 7, the CO_2 release (from Fig. 3a) is shown with a blue line, the green line indicates the conductive heat flow trend (from Fig. 3b), the Moho variations (from Fig. 3c) are shown with a black line, the Bouguer anomalies (from Fig. 3d) with a red line, the seismogenic thickness (from Fig. 4a) with a yellow line, and the red and black vectors indicate the projection of the 3D GNSS velocities along the strike of the profile in two different bins (± 10 and ± 30 km from the profile trace, respectively).

In the NAP profile (Fig. 7a), the pattern of ΔVs is characterized by negative anomalies involving the entire crust except for a region of positive anomalies within the lower crust that correspond with the Moho overlap. Seismicity occurs above 10 km depth beneath the Tyrrhenian domain and the chain axis where a negative ΔVs is imaged (Fig. 7a), while beneath the Adriatic domain earthquake hypocenters deepen to 20-25 km depth. The highest seismic release occurs along the axial belt of the Apennines, slightly shifted eastward with respect to the Moho overlap area where the highest extensional strain-rates are observed. This portion of the profile is also characterized by positive vertical deformation highlighting the general uplift of the chain axis with respect to the null uplift of the Adriatic sector and the subsidence of the Tyrrhenian domain. The Bouguer gravity anomalies show values in the range of +30 to -30 mGal marking the transition from the Tyrrhenian to the Adriatic domain at ~0 mGal (Fig. 3d). The CO_2 flux values as well as the conductive heat flow trend reach their maxima west of the Moho overlap, in the Tyrrhenian domain. Mantle scale shear wave velocities define a large high velocity anomaly located beneath the western portion of the Apennines (Giacomuzzi et al., 2012) depicting the sub-vertical high-

velocity Adriatic slab and the low-velocity mantle wedge, which is particularly pronounced in the topmost 100-120 km below the northern Apennines. This large low ΔVs matches the major CO_2 degassing area of Tuscany where the conductive heat flow distribution (Fig. 3b) reaches values over 150 mWm^{-2}, therefore accounting for a low rate of seismicity and a reduced seismogenic thickness (Fig. 4a). These features reflect the predominant viscous deformation of the crust due to heating and a shallower depth of the elastic to viscous transition with respect to what is observed in the Apennines and Adriatic foreland (Cowie et al., 2013).

Beneath the CAP (Fig. 7b), negative ΔVs are limited to the upper crust, just above the seismogenic thickness, and are locally interrupted by positive anomalies. Conversely, the lower crust is characterized by positive anomalies with the highest values in correspondence of the Moho overlap. The Bouguer anomalies show positive values (up to 30 mGal) in the Tyrrhenian domain and negative values (up to -30 mGal) in the Adriatic domain with a marked transition at the Moho overlap (black line in Fig. 7b). In most of the Tyrrhenian domain the seismicity clusters at the top of the high velocity zone above 10-13 km, although the highest seismic release occurs across the axial belt of the Apennines. Shallow seismicity abruptly vanishes just east of the Moho overlap, becoming deeper (down to 30 km depth, Fig. 7b) and sparse in the rest of the Adriatic domain. Moderate strain-rates (up to 30 nanostrains yr^{-1}) coupled with a general uplift of 1-2 mm yr^{-1} can be observed for a wide portion of the CAP profile, suggesting diffuse deformation across the central Apennines. Crustal deformation occurs also in the western side of the Adriatic domain where seismicity is scarce, therefore suggesting considerable aseismic behavior of the active faults mapped in the region (DISS working group, 2021). In the CAP profile, the sub-vertical high velocity Adriatic slab and the low velocity mantle wedge across the central Apennines are well imaged. The negative ΔVs anomaly beneath the western portion of the NAP profile (Fig. 7a) is also observed in CAP (Fig. 7b) and extends from the Latium volcanic area in the west towards the chain axis in the east and overlaps with the largest degassing area of central Italy, which includes both volcanic and non-volcanic CO_2 emissions. The conductive heat flow distribution (green line in Fig.

7b) reaches values over 100 mWm^{-2} just along the Tyrrhenian coast and drastically reduces to values smaller than 40 mWm^{-2} for the rest of the profile. These values are not representative of the real heat flow distribution over the region, as clearly shown by the advective heat flow measurements carried out in various springs of the central Apennines aquifers (Fig. 7b, black segments), which exhibited values between 170 and 380 mWm^{-2} (Di Luccio et al., 2018; Chiodini et al., 2020, 2021).

In the northern SAP (Fig. 7c), although negative velocity anomalies are imaged in different regions along the whole profile, the largest negative ΔVs are confined to the upper crust in the western half of the profile, while positive ΔVs are found beneath the Gargano region in the eastern sector of nSAP. At the western margin of nSAP, one of the main clusters of seismicity is located between 5 and 15 km depth just east of the Campanian volcanic area (Phlegrean Fields and Vesuvius) beneath the chain axis. Instead, the eastern half of the profile is characterized by diffuse (in space and depth), seismicity that deepens in the Adriatic foreland beneath the Gargano promontory. The extensional strain-rates show two areas of high values that correspond with the Campanian volcanoes and crosses the chain axis (black line in Fig. 7c). The former is characterized by strain-rates up to 65 nanostrain yr^{-1}, coupled with a local uplift of 1-2 mm yr^{-1}, a minimum (6-9 km) seismogenic thickness (yellow line) and a negligible seismic release that reflects the prevailing aseismic deformation of the crust due to the presence of magma pockets at relatively shallow depths (Auger et al., 2001; Mangiacapra et al., 2008). The latter involves a ~65-km-wide belt across the chain axis and shows strain-rates up to 35 nanostrain yr^{-1} in correspondence of the Moho overlap. This sector is also characterized by an uplift (black line in Fig. 7c) of ~3 mm yr^{-1} that progressively decreases eastward approaching the Gargano region. In the Tyrrhenian and Adriatic domains, the Bouguer anomalies show values above 100 mGal that decrease to a minimum of ~30 mGal at the Moho overlap (red line in Fig. 7c). Mantle scale tomography defines a large low velocity anomaly which extends from the Campanian volcanic area in the west to the southern Apennines chain axis in the east and is coincident with the largest degassing area of southern Italy,

which includes the volcanic and non-volcanic CO_2 emission sites (Fig. 7c). The conductive heat flow distribution (green line in Fig. 7c) is generally smaller than 60 mWm^{-2}, although two narrow regions with values over 100 mWm^{-2} can be observed along the chain axis and at the western margin of the Gargano area. The first area coincides with the Irpinia fault zone, whose northern tip coincides with the non-volcanic degassing area of Mefite D'Ansanto (Chiodini et al., 2010), and the second one is found in the crustal thermal source region beneath Candelaro, just south of the Gargano Promontory (Filippucci et al., 2019).

In the central SAP (Fig. 7d), a few small local positive anomalies are present within the large negative ΔVs region in the upper crust beneath the western and central sectors of the profile, while in the eastern sector a large positive anomaly is imaged in the lower crust. In the topmost 60-100 km, mantle scale tomography defines a low-velocity region that extends from the Tyrrhenian coast to the mountain chain. Beneath the Adriatic foreland the high-velocity anomaly extends from crustal to mantle depths where it dips westward beneath the Tyrrhenian region. The Bouguer anomalies (red line in Fig. 7d) are generally positive with a local minimum (~0 mGal) above the Moho overlap. Most of the seismicity occurs above 10-12 km depth defined by the seismogenic thickness (yellow line in Fig. 7d) that sharply deepens eastward beneath the Adriatic domain. The highest seismic release occurs in the region of the Moho overlap spatially matching the distribution of both the highest strain-rate (up to 45 nanostrain yr^{-1}) and uplift values (~2 mm yr^{-1}) across the chain axis (black line and black vectors in Fig. 7d, respectively). Heat flow values (green line in Fig. 7d) are generally low (~50 mWm^{-2}), while CO_2 emissions (blue line in Fig. 7d) show high values only in the westernmost sector of the profile with decreasing values approaching the chain axis. The center of this profile crosscuts the Mount Vulture volcano highlighting its very peculiar location above the mantle wedge, where the Moho decoupling occurs just above the slab tear at depth (Beccaluva et al., 2002; Faccenna et al., 2005; De Astis et., 2006). At Mount Vulture, the R/Ra values reach 6 suggesting a mantle origin for the fluids (Caracausi et al., 2015 and references therein; Minissale et al., 2019).

Beneath the southern SAP (Fig. 7e), negative ΔVs values are confined in a well-defined volume of the upper crust above the Moho overlap, while the lower crust is characterized by positive ΔVs. The Bouguer anomalies (red line in Fig. 7e) are generally positive with minima (~ -50 mGal) slightly east of the Moho overlap. Most of the seismicity is focused on the western edge of the negative ΔVs volume at shallow depth and in close correspondence with the highest extensional strain-rates (up to 25 nanostrains yr^{-1}, black line in Fig. 7e). Along the remaining part of the profile, seismicity is scarce and characterized by slightly deeper hypocenters. The highest extensional strain-rates mark the transition from small vertical motions (generally < 0.8 mm yr^{-1}) on the Tyrrhenian side, up to 2 mm yr^{-1} across the central sector of the profile and null vertical motion occurs only on the Apulian coastal margin. The mantle scale tomography is generally characterized by high wave speed anomalies, while low ΔVs are imaged only at depths greater than 100 km below the Apulian foreland. These features highlight the absence of a mantle wedge beneath this part of the southern Apennines, therefore suggesting a thermal structure of the whole lithosphere not influenced by the mantle wedge and in agreement with the measured low heat flow values (~50 mWm^{-2}).

Some key features emphasising the complexity of the Apennines framework arise from our analysis of the different datasets. The first feature is the presence of a westward subducting Adriatic slab clearly imaged below 100 km depth beneath most of the Apennines although fragmented between 100 km and 250 km depth (Fig. 6), as already observed in several tomographic models (Lucente et al., 1999; Wortel and Spakman, 2000; Piromallo and Morelli, 2003; Giacomuzzi et al., 2012; Magnoni et al., 2022). The tomographic model used in our study (Giacomuzzi et al., 2012) images a wide region of negative ΔVs extending above 100-km depth from the NAP near Larderello to central SAP near Mefite d'Ansanto (Fig. 6). This broad low-velocity anomaly is interpreted as an asthenospheric flow through the slab window, which developed as a consequence of the tearing of the Adriatic slab (Giacomuzzi et al., 2012 and references therein). At shallow depths the large hot asthenospheric wedge intrudes between the overriding Tyrrhenian lithosphere

and the subducting Adriatic slab. This is also found in the recent full waveform tomography model by Magnoni et al. (2022) that depicts a low Vs and high Vp/Vs below 20 km depth between 70 to 120 km along a SW-NE profile running from Tuscany to the Adriatic Sea. Beneath the central Apennines, the eastward and upward intrusion of the asthenospheric wedge would be responsible for both the crustal thinning and the long-wavelength uplift areas of the chain axis, as already suggested by D'Agostino et al. (2001), and confirmed by the Plio-Quaternary intermountain basins associated with the prevailing vertical deformation (Cowie et al., 2017). The hot asthenospheric wedge is likely responsible for the thermal structure of the back-arc region and affects the rheological strength of the lithologies, metamorphism, dehydration reactions and melting that occur in the downgoing lithosphere. Regarding the rheological aspect, the mantle wedge produces high heat flow at the surface in the CDS and in the large area encompassing the geothermal and volcanic sectors of the TRDS. The high heat flow favors a prevalent viscous deformation of the crust accounting for the observed reduced seismogenic thickness (Fig. 4a). We note that the conductive heat flow values do not take into account the advective heat flow measurements carried out in the large aquifers of the study region. The advective heat flow values estimated in these aquifers are comparable to those of TRDS and CDS (Di Luccio et al., 2018; Chiodini et al., 2020, 2021). The partial melting of the subducting lithosphere produces magmatic melts that uprise to the surface through the overriding stretched lithosphere. Along the Tyrrhenian side, the rising of magmatic melts has produced Plio-Quaternary shallow intrusions and subaerial NW-SE aligned volcanoes (Peccerillo and Lustrino, 2005) with ages generally decreasing from Tuscany (TRDS) south-eastward to the CDS (Fig. 1c). At present, geothermal sources dominate in TRDS, and volcanoes in the Tuscany and Latium regions are no longer active although still in a quiescent stage (Albani Hills last eruption 36ka, Trasatti et al., 2018). Instead, to the southeast, the presence of the active Phlegrean Fields and Vesuvius volcanoes in CDS is possibly related to the larger crustal stretching in the southern Tyrrhenian domain (Rosenbaum and Lister, 2004).

The melting process involves most of the lithologies of the upper Adriatic crust, characterized by a large compositional variability with a predominance of carbonate-rich rocks (up to 10 km thick) in the foreland as indicated in outcrops. Partial melting of these subducted lithologies occurs at 60-130 km depth corresponding to a temperature of ~1260° C (Frezzotti et al., 2009) and metasomatizes the mantle wedge, favoring a continuous CO_2 flux from about 60 km depth to the surface. This geodynamic context is supported as well by the measured ^{238}U excess in Vesuvius lavas (Avanzinelli et al., 2018), whose values require a mantle source with the addition of U-rich carbonated melts that are related to the partial melting of the subducted carbonate sedimentary rocks. Avanzinelli et al. (2018) estimate a flux of 0.15-0.8 Mt yr^{-1} of CO_2 from the subducted carbonates to the mantle source of Mount Vesuvius.

The diffuse deeply-derived CO_2-rich fluids correspond to the TRDS to the north and the CDS to the south. High values of deep-source CO_2 are also measured in the central and southern Apennines, in the Velino and Sannio-Matese aquifers, respectively (Chiodini et al., 2020; Di Luccio et al., 2018). In these two aquifers thousands of liters per second of CO_2-rich waters as well as hundreds of liters per second of CO_2-oversaturated waters and direct emissions of a CO_2-rich gas phase have been measured (Di Luccio et al., 2018; Chiodini et al., 2020). The increasing R/Ra values (> 0.4) from the northern to the southern Apennines reflects a decreasing degree of metasomatism of the asthenospheric wedge, possibly associated with a different composition and thickness of the subducted lithosphere (Minissale et al., 2019). The very low R/R_a values (of 0.1-0.2) and the absence of deep-source CO_2 in groundwaters beneath the Pollino region clearly support the lack of a mantle component there and the prevailing crustal source of the emitted gasses (Apollaro et al., 2020).

The primary role of CO_2-rich fluids has been proven in the earthquake triggering mechanism as well as in the evolution of the seismic sequences of the Apennines, such as the 1997-1998 Umbria-Marche seismic sequence in the northern Apennines (Miller et al., 2004), the 2009 L'Aquila (Di Luccio et al., 2010; Lucente et al., 2010; Terakawa et al., 2010; Malagnini et al.,

2012) and the 2016-2017 Amatrice-Norcia earthquakes (Chiarabba et al., 2020; Gunatilake and Miller, 2022) in the central Apennines, the 2013-2014 Sannio-Matese (Di Luccio et al., 2018) and the 2010-2014 Pollino seismic swarm-like sequence (Napolitano et al., 2020; De Matteis et al., 2021) in the southern Apennines. The common feature of these sequences is the prevalent normal faulting mechanism coupled with the presence of overpressurized CO_2-rich fluids reservoirs at depth. Based on the available data, the size of these reservoirs deduced from seismological studies ranges from ~$0.4 \cdot 10^3$ km^3 (in the Irpinia region, Amoroso et al., 2014) to ~$6 \cdot 10^3$ km^3 (in the central Apennines, Chiodini et al., 2011) with the top at ~5-6 km depth (Chiarabba et al., 2018). In the Campanian Apennines, hydrocarbon exploration data and local earthquake tomography images suggest the existence of CO_2-rich fluids reservoirs at different structural levels within the Apulia Carbonate Platform (Improta et al., 2014): relatively shallow aqueous reservoirs with CO_2 pressurized gas caps drilled at 1-3 km depth at the top of anticlines, and CO_2-rich fluid reservoirs at the base of the Apulian carbonates inferred by velocity anomalies (Improta et al., 2014; Chiodini et al., 2010; Amoroso et al., 2014; Amoroso et al., 2017). Mio-Pliocene clay-rich turbidites and Triassic anhydrites would act as cap-rock horizons of the shallow and deep reservoirs, respectively.

Besides other poorly constrained causative sources such as creeping or blind faults, along the Apennines the crustal deformation associated with these overpressurized fluid reservoirs could partially balance the total geodetic deformation budget, therefore providing a possible explanation for the observed deficit in seismic strain (Pondrelli, 1999; Hunstad et al., 2003; Palano et al., 2011; Carafa et al., 2020). Beneath the Tyrrhenian side of the Apennines, the reduced crustal thickness, the high permeability (Ghisetti and Vezzani, 2002), and the shallow brittle-ductile transition do not support the formation of pressurized reservoirs. Conversely, the presence of a thickened and less permeable crust beneath the axial mountain belt, coupled with the thickening of the seismogenic layer, lead to restricted fluid circulation toward the surface and favors the creation of overpressurized reservoirs at depth. In this area, extensional faults act as episodic high-permeability pathways during seismic activity. As a result, the thickness of the crust as well as its permeability

control the formation of overpressurized fluid zones at depth and thus the seismicity. In the southern Apennines, seismicity is deeper, earthquakes with magnitude larger than 6.5 occur along NW-SE striking faults, and high heat flow is mainly associated with the upward migration of CO_2-rich fluids along pre-existing and active faults and the occurrence of magmatic intrusions (Sannio-Matese, Mount Vulture). In fact, the southern Apennines show evidence of pressurized fluid-rich zones and possible intrusions at depths of 10-15 km, a depth interval significantly deeper than that of the intrusions in Tuscany (Di Luccio et al., 2018; Chiarabba et al., 2020). While in the Apennines the magnitude and number of events are modulated by the mantle CO_2 uprise, in the Pollino area the lack of CO_2 release time series does not allow us to compare the gas emission trend to the seismicity rate with detail, despite the accepted role of overpressurized fluids in the seismogenic process in this region (De Matteis et al., 2021). Nevertheless, these observations allow us to suggest that the origin of these fluids in the Pollino area is the shallow crust.

Away from the axis of the Apennines, seismic sequences generally occur on deep and blind faults and are not related to overpressurized fluids, as for instance the 1990-91 M_w5.7 Potenza (Di Luccio et al., 2005b) and the 2002 M_w5.8 Molise (Pino and Di Luccio, 2005; Di Luccio et al., 2005a; Vallée and Di Luccio, 2005). This feature coupled with the null CO_2 release at the surface proves that the off-axis seismicity is not linked to gas emissions and suggests that in the Adriatic plate, earthquake nucleation occurs at lithostatic pore-pressure conditions. An exception is the 2012 M_w5.8 Emilia earthquake in the northern Apennines, where the activation of buried thrusts was driven by fluid overpressure pulses at the base of the carbonate sequence (Calderoni et al., 2009; Ventura and Di Giovambattista, 2013; Pezzo et al., 2018).

This work highlights how the melting of the sedimentary cover of the subducting plate and the resulting fluid release into the upper mantle and overlying crust may create overpressurized storage zones, which in turn are able to produce deformation at the surface and trigger shallow seismicity. This mechanism can be exported to different tectonic settings, including the central

Europe rift (Mousavi et al., 2015), NE China (Zhang et al., 2019) and southeastern Tibetan Plateau (Zhang et al., 2021).

7. Conclusions

We provided an updated overview of the fluids and seismicity relationships in the Apennines through a multidisciplinary approach, by discussing the geodynamic setting of the region, correlating and interpreting the CO_2 distribution with several geophysical datasets from the literature and novel observations. At the scale of the Apennines, our analysis allows us to highlight differences between the western and eastern domains, in terms of Moho depth, Bouguer gravity anomalies, seismicity distribution, seismogenic thickness, tomographic Vs and Vp/Vs anomalies, CO_2 release and heat flow patterns. The transition zone between the Adriatic and Tyrrhenian domains is characterized by high seismic release and geodetic strain, prevailing uplift, Moho overlap, and mantle wedge intrusion at depth.

The main findings are summarized below:

- The Apennines seismicity is shallow (above 10-15 km depth) and confined within a ~50 km strip along the chain axis where active faults are NW-SE striking. Here the most destructive earthquakes (M>6.5) and seismic sequences have occurred in the past. In the Apulian foreland, sparse, deeper (down to 35 km depth), moderate-magnitude earthquakes depict an E-W trending belt related to a deep tectonic discontinuity. On the Tyrrhenian side, seismicity is arranged in spot-like clusters located in the volcanic and geothermal areas of Tuscany, Latium, and Campania. Low frequency seismic events and transient signals, related to fluid movements, are also recorded in the northern and central Apennines.
- CO_2-rich fluids stored in the crust play a major role in triggering seismicity by diffusive processes and in modulating the space-time evolution of the major sequences of the Apennines.
- The Tyrrhenian-northern Apennines domain is characterized by intense crustal stretching, a relatively shallow Moho, low seismic release, volcanic and geothermal areas, crustal

magmatic intrusions, high conductive heat flow, and CO_2 release. The highest extensional strain-rates occur beneath the chain axis where most of the active extensional faults are the loci of destructive earthquakes. The Adriatic edge of the northern Apennines is characterized by null uplift, scant and deep (>20 km depth) seismicity with strike-slip to reverse focal mechanisms.

- The Tyrrhenian domain of the central Apennines is marked by an extended zone of high CO_2 release, high conductive heat flow, and seismicity shallower than ~15 km. The highest seismic release occurs across the axial belt of the Apennines, while eastward earthquakes are scarce and deeper (~30 km depth). Diffuse horizontal deformation coupled with general uplift characterizes a wide portion of the central Apennines.
- Dense and shallow seismicity occurs beneath the southern Apennines chain axis at its northern tip; seismicity becomes sparse and deeper moving eastward to the Adriatic coast. The largest values of seismic release, strain accumulation and uplift are recorded beneath the chain axis of the southern Apennines. The seismogenic thickness in the Campanian volcanic area is very thin, and the small seismic release coupled with the high strain-rate suggests prevailing aseismic deformation of the crust. The major areas of volcanic and non-volcanic CO_2 release concentrate in the CDS and some portions of the mountain chain. The conductive heat flow exhibits two significant local maxima: the first one is in the Irpinia fault zone, whose northern tip hosts the largest non-volcanic degassing site of Mefite d'Ansanto, and the second one is located beneath the crustal geothermal source of Candelaro, just south of the Gargano Promontory. In contrast, beneath the central portion of the southern Apennines, heat flow values are generally low, while the CO_2 release shows high values off the chain axis. In the southernmost portion of the southern Apennines, the highest extensional strain-rates mark the transition from small vertical motions on the Tyrrhenian side to significant uplift across the chain axis and null vertical motions on the Apulian coastal margin. In this portion of the southern Apennines, the low heat flow values

indicate a lithosphere with a thermal structure typical of stable continental regions, as also confirmed by the lack of a mantle wedge and emissions of deep fluids at the surface.

- The intruding hot asthenospheric mantle wedge beneath the Apennines regulates the thermal structure and rheology of the overlying crust and is responsible for the melting of the carbonate-rich sediments of the subducting Adriatic lithosphere.
- The different degree of metasomatism of the asthenospheric mantle wedge decreases from the northern to the southern Apennines along with differences in the composition and thickness of carbonate-rich lithologies in the subducted lithosphere; the mantle wedge disappears beneath the Pollino massif, at the southern edge of the southern Apennines, where the dissolved fluids have a prevalent crustal origin.

To date, the lack of a multiparametric monitoring system and of the long-term analysis of different geophysical and geochemical observables has prevented the formulation of any comprehensive, data-constrained, reliable conceptual model on the role of fluids in the preparatory phase of earthquakes in southern Apennines. This study strongly relies on the multidisciplinary analysis of different datasets (both existing and newly acquired) with the most advanced methodologies to stimulate the knowledge of the fluid-related mechanisms of earthquake preparation, nucleation and space-time evolution. Ongoing and future investigations will include the continuous and simultaneous geochemical and geophysical monitoring at the scale of the outcropping seismogenic faults to properly decipher the link between earthquake occurrence, surface rupture and fluid release.

Acknowledgements

Fabrizio Balsamo and two anonymous reviewers are thanked for their constructive comments that improved the manuscript. Gillian R. Foulger is acknowledged for the editorial management of the

manuscript. This work was supported by the Istituto Nazionale di Geofisica e Vulcanologia and funded by the Earthquake Department Strategic Project FURTHER "The role of FlUids in the pReparaTory pHase of EaRthquakes in Southern Apennines". All authors are part of the FURTHER Team. The GNSS data used in this study were processed in the Task S4 of the INGV Project: 'Pianeta Dinamico (Dynamic Planet)-Working Earth': Geosciences For The Understanding The Dynamics Of The Earth And The Consequent Natural Risks, funded by the Ministry of University and Research. All figures were produced with the GMT software (Wessel et al., 2019).

References

Agricola, G., 1556. De Re Metallica, Translated by H.C. and L.H. Hoover, Dover, Mineola, New York.

Amoroso, O., Ascione, A., Mazzoli, S., Virieux, J., Zollo, A., 2014. Seismic imaging of a fluid storage in the actively extending Apennine mountain belt, southern Italy. Geophys. Res. Lett. 41, 3802-3809. https://doi.org/10.1002/2014GL060070.

Amoroso, O., Russo, G., De Landro, G., Zollo, A., Garambois, S., Mazzoli, S., Parente, M., Virieux, J., 2017. From velocity and attenuation tomography to rock physical modeling: Inferences on fluid-driven earthquake processes at the Irpinia fault system in southern Italy. Geophys. Res. Lett. 44, 6752-6760. https://doi.org/10.1002/2016GL072346.

Anzidei, M., Baldi, P., Casula, G., Galvani, A., Mantovani, E., Pesci, A., Riguzzi, F., Serpelloni, E., 2001. Insights into present-day crustal motion in the central Mediterranean area from GPS surveys. Geophys. J. Int. 146, 98-110. https://doi.org/10.1046/j.0956-540x.2001.01425.x.

Apollaro, C., Caracausi, A., Paternoster, M., Randazzo, P., Aiuppa, A., De Rosa, R., Fuoco, I., Mongellice, G., Muto, F., Vannia, E., Vespasiano, G., 2020. Fluid geochemistry in a low-enthalpy geothermal field along a sector of southern Apennines chain Italy. J. Geochem. Explor. 219, 106618. https://doi.org/10.1016/j.gexplo.2020.106618.

Ascione, A., Ciotoli, G., Bigi, S., Buscher, J., Mazzoli, S., Ruggiero, L., Sciarra, A., Tartarello, M.C., Valente, E., 2018. Assessing mantle versus crustal sources for non-volcanic degassing

along fault zones in the actively extending Southern Apennines mountain belt (Italy). GSA Bull. 130, 9-10. https://doi.org/10.1130/B31869.1.

Auger, E., Gasparini, P., Virieux, J., Zollo, A., 2001. Seismic evidence of an extended magmatic sill under Mt. Vesuvius. Science 294, 1510-1512. https://doi.org/10.1126/science.1064893.

Avanzinelli, R., Casalini, M., Elliott, T., Conticelli, S., 2018. Carbon fluxes from subducted carbonates revealed by uranium excess at Mount Vesuvius, Italy. Geology 46 (3), 259-262. https://doi.org/10.1130/G39766.1.

Bagagli, M., Kissling, E., Piccinini, D., Saccorotti, G., 2020. Local earthquake tomography of the Larderello-Travale geothermal field. Geothermics 83, 101731. https://doi.org/10.1016/j.geothermics.2019.101731.

Bally, A.W., Burbi, L., Cooper, C., Ghelardoni, R., 1986. Balanced sections and seismic reflection profiles across the central Apennines. Mem. Soc. Geol. Ital. 35, 257-310.

Barchi, M. R., 2010. The Neogene-Quaternary evolution of the Northern Apennines: crustal structure, style of deformation and seismicity. In: Beltrando, M., Peccerillo, A., Mattei, M., Conticelli, S., Doglioni, C. (Eds.), J. Virt. Explor. The Geology of Italy: Tectonics and Life Along Plate Margins, 36, pp. 1-24

Barchi, M., Minelli, G., Magnani, B., Mazzotti, A., 2003. Line CROP 03: Northern Apennines. Mem. Descr. Carta Geol. d'It. LXII.

Barchi, M.R., Alvarez, W., Shimabukuro, D.H., 2012. The Umbria-Marche Apennines as a Double Orogen: Observations and hypotheses. Ital. J. Geosci. 131 (2), 258-271. https://doi.org/10.3301/IJG.2012.17.

Barnes, I., Irwin, P.W., White, D.E., 1978. Global Distribution of Carbon Dioxide Discharges, and Major Zones of Seismicity, in: Barnes, I., Irwin, W.P., White, D.E. (Eds.), Water Resources Investigation WRI 78-39, U.S. Geological Survey, Washington, pp 1-17. https://doi.org/10.3133/wri7839.

Beccaluva, L., Coltorti, M., Di Girolamo, P., Melluso, L., Milani, L., Morra, L., Siena, F., 2002. Petrogenesis and evolution of Mt. Vulture alkaline volcanism (southern Italy). Mineral. Petrol. 74, 277-297. https://doi.org/10.1007/s007100200007.

Bennett, R.A., Serpelloni, E., Hreinsdóttir, S., Brandon, M.T., Buble, G., Basic, T., Casale, G., Cavaliere, A., Anzidei, M., Marjonovic, M., Minelli, G., Molli, G., Montanari, A., 2012. Syn-convergent extension observed using the RETREAT GPS network, northern Apennines, Italy. J. Geophys. Res. 117, B04408. https://doi.org/10.1029/2011JB008744.

Bonini, L., Toscani, G., Seno, S., 2014. Three-dimensional segmentation and different rupture behavior during the 2012 Emilia seismic sequence (northern Italy). Tectonophysics 630, 33-42. https://doi.org/10.1016/j.tecto.2014.95.006.

Bräuer, K., Kämpf, H., Strauch, G., Weise, S., 2003. Isotopic evidence ($^{3}He/^{4}He$,$^{13}C_{CO2}$) of fluid-triggered intraplate seismicity. J. Geophys. Res. 108, https://doi.org/10.1029/2002JB002077.

Butler, R.W.H., Mazzoli, S., Corrado, S., De Donatis, M., Di Bucci, D., Gambini, R., Naso, G., Nicolai, C., Scrocca, D., Shiner, P., Zucconi, V., 2004. Applying thick-skinned tectonic model to the Apennine thrust-belt of Italy: Limitations and implications, in: McClay, K.R. (Eds.), Thrust Tectonic and Hydrocarbon System., Mem. AAPG, 82, pp. 647-667. https://doi.org/10.1306/M82813.

Calderoni, G., Di Giovambattista, R., Burrato, P., Ventura, G., 2009. A seismic sequence from Northern Apennines (Italy) provides new insight on the role of fluids in the active tectonics of accretionary wedges. Earth Planet. Sci. Lett. 281 (1-2), 99-109. https://doi.org/10.1016/j.epsl.2009.02.015.

Calderoni, G., Rovelli, A., Di Giovambattista, R., 2015. Transient anomaly in fault zone-trapped waves during the preparatory phase of the 6 April 2009, Mw 6.3 L'Aquila earthquake. Geophys. Res. Lett. 42 (6), 1750-1757. https://doi.org/10.1002/2015GL063176.

Calò, M., Dorbath, C., Luzio, D., Rotolo, S. G., D'Anna, G., 2012. Seismic velocity structures of southern Italy from tomographic imaging of the Ionian slab and petrological inferences. Geophys. J. Int. 191 (2), 751-764. https://doi.org/10.1111/j.1365-246X.2012.05647.x.

Cambiotti, G., Palano, M., Orecchio, B., Marotta, A.M., Barzaghi, R., Neri, G., Sabadini, R., 2020. New Insights into Long-Term Aseismic Deformation and Regional Strain Rates from GNSS Data Inversion: The Case of the Pollino and Castrovillari Faults. Remote Sens. 12, 2921. https://doi.org/10.3390/rs12182921.

Caracausi, A., Martelli, M., Nuccio, P.M., Paternoster, M., Stuart, F.M., 2013. Active degassing of mantle-derived fluid: A geochemical study along the Vulture line, southern Apennines (Italy). J. Volcanol. Geotherm. Res. 253, 65-74. https://doi.org/10.1016/j.jvolgeores.2012.12.005.

Caracausi, A., Paternoster, M., Nuccio, P.M., 2015. Mantle CO_2 degassing at Mt. Vulture volcano (Italy): Relationship between CO_2 outgassing of volcanoes and the time of their last eruption. Earth Planet. Sci. Lett. 411, 268-280, https://doi.org/10.1016/j.epsl.2014.11.049.

Carafa, M. M. C., Galvani, A., Di Naccio, D., Kastelic, V., Di Lorenzo, C., Miccolis, S., Sepe, V., Pietrantonio, G., Gizzi, C., Mastrucci, A., Valensise, G., Bird, P., 2020. Partitioning the ongoing extension of the central Apennines (Italy): Fault slip rates and bulk deformation rates from geodetic and stress data. J. Geophys. Res. 125, e2019JB018956. https://doi.org/10.1029/2019JB018956.

Carafa, M. M. C., Valensise, G., Bird, P., 2017. Assessing the seismic coupling of shallow continental faults and its impact on seismic hazard estimates: a case-study from Italy. Geophys. J. Int. 209 (1), 32-47. https://doi.org/10.1093/gji/ggx002 .

Carmignani, L., Kligfield, R., 1990. Crustal extension in the northern Apennines: the transition from compression to extension in the Alpi Apuane core complex. Tectonics 9, 1275-1303. https://doi.org/10.1029/TC009i006p01275.

Carmignani, L., Decandia, F. A., Fantozzi, P. L., 1994. Tertiary extensional tectonics in Tuscany (Northern Apennines, Italy). Tectonophysics, 238, 295-315. https://doi.org/10.1016/0040-1951(94)90061-2.

Casero, P., Roure, F., Endignoux, L., Moretti, I., Muller, C., Sage, L., Vially, R., 1988. Neogene geodynamic evolution of the Southern Apennines. Mem. Soc. Geol. It. 41, 109-120.

Cassinis, R., Scarascia, S., Lozej, A., 2003. The deep crustal structure of Italy and surrounding areas from seismic refraction data; a new synthesis. Boll. Soc. Geol. Ital. (Ital. J. Geosci.) 122 (3), 365-376.

Catalano, S., C. Monaco, C., Tortorici, L., Paltrinieri, W., Steel, N., 2004. Neogene-Quaternary tectonic evolution of the southern Apennines. Tectonics 23, TC2003, https://doi.org/10.1029/2003TC001512.

Cataldi, R., Mongelli, F., Squarci, P., Taffi, L., Zito, G., Calore, C., 1995. Geothermal ranking of Italian Territory. Geothermies 1(24), 115-129. https://doi.org/10.1016/0375-6505(94)00026-9.

Cello, G., Mazzoli, S., 1999. Apennine tectonics in Southern Italy: a review. J. Geodyn. 27, 191-211. https://doi.org/10.1016/S0264-3707(97)00072-0.

Channell, J.E.T., D'Argenio, B., Horvath, F., 1979. Adria, the African Promontory, in Mesozoic Mediterranean paleogeography. Earth-Sci. Rev. 15, 213-292. https://doi.org/10.1016/0012-8252(79)90083-7.

Chiarabba, C., Jovane, L., Di Stefano, R., 2005. A new view of Italian seismicity using 20 years of instrumental recordings. Tectonophysics 395 (3-4), 251-268. https://doi.org/10.1016/j.tecto.2004.09.013.

Chiarabba, C., De Gori, P., 2016. The seismogenic thickness in Italy: constraints on potential magnitude and seismic hazard. Terra Nova 28, 402-408. https://doi.org/10.1111/ter.12233.

Chiarabba, C., Palano, M., 2017. Progressive migration of slab break-off along the southern Tyrrhenian plate boundary: Constraints for the present day kinematics. J. Geodyn. 105, 51-61. https://doi.org/10.1016/j.jog.2017.01.006.

Chiarabba, C., De Gori, P., Cattaneo, M., Spallarossa, D., Segou, M., 2018. Faults Geometry and the Role of Fluids in the 2016–2017 Central Italy Seismic Sequence. Geophys. Res. Lett. 45, 14. https://doi.org/10.1029/2018GL077485.

Chiarabba, C., Bianchi, I., De Gori, P., Piana Agostinetti, N., 2020. Mantle upwelling beneath the Apennines identified by receiver function imaging. Sci. Rep. 10, 19760. https://doi.org/10.1038/s41598-020-76515-2.

Chiodini, G., Frondini, F., Cardellini, C., Parello, F., Peruzzi, L., 2000. Rate of diffuse carbon dioxide Earth degassing estimated from carbon balance of regional aquifers: the case of central Apennine, Italy. J. Geophys. Res. 105, 8423-8434. https://doi.org/10.1029/1999JB900355.

Chiodini, G., Cardellini, C., Amato, A., Boschi, E., Caliro, S., Frondini, F., Ventura, G., 2004. Carbon dioxide Earth degassing and seismogenesis in central and southern Italy. Geophys. Res. Lett. 31, L07615, https://doi.org/10.1029/2004GL019480.

Chiodini, G., Granieri, D., Avino, R., Caliro, S., Costa, A., Minopoli, C., Vilardo, G., 2010. Non-volcanic CO_2 Earth degassing: Case of Mefite d'Ansanto (southern Apennines), Italy. Geophys. Res. Lett. 37, L11303. https://doi.org/10.1029/2010GL042858.

Chiodini, G., Caliro, S., Cardellini, C., Frondini, F., Inguaggiato, S., Matteucci, F., 2011. Geochemical evidence for and characterization of CO_2 rich gas sources in the epicentral area of the Abruzzo 2009 earthquakes. Earth Planet. Sci. Lett. 304 (3-4), 389-398. https://doi.org/10.1016/j.epsl.2011.02.016.

Chiodini, G., Cardellini, C., Di Luccio, F., Selva, J., Frondini, F., Caliro, S., Rosiello, A., Beddini, G., Ventura, G., 2020. Correlation between tectonic CO2 Earth degassing and seismicity is

revealed by a 10-year record in the Apennines, Italy. Sci. Adv. 6 (35). https://www.science.org/doi/10.1126/sciadv.abc2938.

Chiodini, G., Cardellini, C., Bini, G., Frondini, F., Caliro, S., Ricci, L., Lucidi, B., 2021. The Carbon Dioxide Emission as Indicator of the Geothermal Heat Flow: Review of Local and Regional Applications with a Special Focus on Italy. Energies 14, 6590. https://doi.org/10.3390/en14206590.

Ciotoli, G., Bigi, S., Tartarello, C., Sacco, P., Lombardi, S., Ascione, A., Mazzoli, S., 2014. Soil gas distribution in the maincoseismic surface rupture zone of the 1980, Ms= 6.9, Irpinia earthquake (southern Italy). J. Geophys. Res. Solid Earth 119, 2440-2461, https://doi.org/10.1002/2013JB010508.

Civile, D., Lodolo, E., Accettella, D., Geletti, R., Ben-Avraham, Z., Deponte, M., Facchin, L., Ramella, R., Romeo, R., 2010. The Pantelleria graben (Sicily Channel, Central Mediterranean): an example of intraplate 'passive' rift. Tectonophysics 490 (3-4), 173-183. https://doi.org/10.1016/j.tecto.2010.05.003.

Cocco, M., Pacor, F., 1993. The rupture process of the 1980 Irpinia, Italy, earthquake from the inversion of strong motion waveforms. Tectonophysics 218 (1-3), 157-177. https://doi.org/10.1016/0040-1951(93)90266-M.

Cosentino, D., Cipollari, P., Marsili, P., Scrocca, D., 2010. Geology of the central Apennines: a regional review. In: Beltrando, M., Peccerillo, A., Mattei, M., Conticelli, S., Doglioni, C. (Eds.), The Geology of Italy: tectonics and life along plate margins. J. Virt. Explor., Electronic Edition, 36. https://doi.org/10.3809/jvirtex.2010.00223.

Cowie, P., Phillips, R., Roberts, G., McCaffrey, K., Zijerveld, L.J.J., Gregory, L.C., Faure Walker, J., Wedmore, L.N.J., Dunai, T.J., Binnie, S.A., Freeman, S.P.H.T., Wilcken, K., Shanks, R.P., Huismans, R.S., Papanikolaou, I., Michetti, A.M., Wilkinson, M., 2017. Orogen-scale uplift in the central Italian Apennines drives episodic behaviour of earthquake faults. Sci. Rep. 7, 44858. https://doi.org/10.1038/srep44858.

Cowie, P.A., Scholz, C.H., Roberts, G.P., Faure Walker, J.P., Steer, P., 2013. Viscous roots of seismogenic faults revealed by geologic slip-rate variations. Nat. Geosci. 6, 1036-1040. https://doi.org/10.1038/ngeo1991.

D'Agostino, N., Jackson, J.A., Dramis, F., Funiciello, F., 2001. Interactions between mantle upwelling, drainage evolution and active normal faulting: an example from the central Apennines (Italy). Geophys. J. Int. 147, 475-497. https://doi.org/10.1046/j.1365-904246X.2001.00539.x.

D'Agostino, N., Avallone, A., Cheloni, D., D'Anastasio, E., Mantenuto, S., Selvaggi, G., 2008. Active tectonics of the Adriatic region from GPS and earthquake slip vectors. J. Geophys. Res., 113, B12413. https://doi.org/10.1029/2008JB005860

D'Agostino, N., Mantenuto, S., D'Anastasio, E., Avallone, A., Barchi, M., Collettini, C., Radicioni, F., Stoppini, A., Fastellini, G., 2009. Contemporary crustal extension in the Umbria-Marche Apennines from regional CGPS networks and comparison between geodetic and seismic deformation. Tectonophysics 476 (1-2), 3-12. https://doi.org/10.1016/j.tecto.2008.09.033.

D'Agostino, N., 2014. Complete seismic release of tectonic strain and earthquake recurrence in the Apennines (Italy). Geophys. Res. Lett. 41 (4), 1155-1162. https://doi.org/10.1002/2014GL059230.

D'Auria, L., Massa, B., De Matteo, A., 2014. The stress field beneath a quiescent stratovolcano: The case of Mount Vesuvius. Geophys. Res. Lett. 119, 1181-1199. https://doi.org/10.1002/2013JB010792.

De Astis, G., Kempton, P.D., Peccerillo, A., Wu, T.W., 2006. Trace element and isotopic variations from Mt. Vulture to Campanian volcanoes: constraints for slab detachment and mantle inflow beneath southern Italy. Contrib. Mineral. Petrol. 151, 331-351. https://doi.org/10.1007/s00410-006-0062-y.

De Landro, G., Amoroso, O., Russo, G., D'Agostino, N., Esposito, R., Emolo, A., Zollo, A., 2022. Decade-long monitoring of seismic velocity changes at the Irpinia fault system (southern

Italy) reveals pore pressure pulsations. Sci. Rep. 12, 1247. https://doi.org/10.1038/s41598-022-05365-x.

De Matteis, R., Convertito, V., Napolitano, F., Amoroso, O., Terakawa, T., Capuano, P., 2021. Pore Fluid Pressure Imaging of the Mt. Pollino Region (Southern Italy) From Earthquake Focal Mechanisms. Geophys. Res. Lett. 48, e2021GL094552. https://doi.org/10.1029/2021GL094552.

Della Vedova, B., Bellani, S., Pellis, G., Squarci, P., 2001. Deep temperatures and surface heat flow distribution, in: Vai, G.B., Martini, I.P. (Eds.), Anatomy of an Orogen: The Apennines and Adjacent Mediterranean Basins. Kluwer Acad. Publ., Dordrecht, pp. 65-76.

Devoti, R., D'Agostino, N., Serpelloni, E., Pietrantonio, G., Riguzzi, F., Avallone, A., Cavaliere, A., Cheloni, D., Cecere, G., D'Ambrosio, C., Franco, L., Selvaggi, G., Metois, M., Esposito, A., Sepe, V., Galvani, A., Anzidei, M., 2017. A Combined Velocity Field of the Mediterranean Region. Ann. Geophys. 60 (2), S0215. https://doi.org/10.4401/ag-7059.

Dewey, J.F., Helman, M.L., Turco, E., Hutton, D.H.W., Knott, S.D., 1989. Kinematics of the Western Mediterranean, in: Coward, M.P., Dietrich, D., Park, R.G. (Eds.), Alpine Tectonics. Geological Society, London, UK. 45, pp. 265-283.

Di Bucci, D., Ridente, D., Fracassi, U., Trincardi, F., Valensise, G., 2009. Marine palaeoseismology from very high resolution seismic imaging: The Gondola Fault Zone (Adriatic foreland). Terra Nova 21, 393-400. https://doi.org/10.1111/j.1365-3121.2009.00895.x.

Di Luccio, F., Fukuyama, E., Pino, N.A., 2005a. The 2002 Molise earthquake sequence: What can we learn about the tectonics of southern Italy? Tectonophysics 405 (1-4), 141-154. https://doi.org/10.1016/j.tecto.2005.05.024.

Di Luccio, F., Piscini, A., Pino, N.A., Ventura, G., 2005b. Reactivation of deep faults beneath Southern Apennines: evidence from the 1990-1991 Potenza seismic sequences. Terra Nova. 17, 586-590. https://onlinelibrary.wiley.com/doi/abs/10.1111/j.1365-3121.2005.00653.x.

Di Luccio, F., Ventura, G., Di Giovambattista, R., Piscini, A., Cinti, F.R., 2010. Normal faults and thrusts reactivated by deep fluids: The 6 April 2009 Mw 6.3 L'Aquila earthquake, central Italy. J. Geophys. Res. 115, B06315. https://doi.org/10.1029/2009JB007190.

Di Luccio, F., Chiodini, G., Caliro, S., Cardellini, C., Convertito, V., Pino, N.A., Tolomei, C., Ventura, G., 2018. Seismic signature of active intrusions in mountain chains. Sci. Adv. 4 (1). https://www.science.org/doi/10.1126/sciadv.1701825.

Di Stefano, R., Kissling, E., Chiarabba, C., Amato, A., Giardini, D., 2009. Shallow subduction beneath Italy: Three-dimensional images of the Adriatic-European-Tyrrhenian lithosphere system based on high-quality P wave arrival times. J. Geophys. Res. Solid Earth 114 (B5), B05305. https://doi.org/10.1029/2008JB005641.

Di Stefano, R., Bianchi, I., Ciaccio, M.G., Carrara, G., Kissling, E., 2011. Three-dimensional Moho topography in Italy: New constraints from receiver functions and controlled source seismology. Geochem. Geophys. Geosys. 12, Q09006. https://doi.org/10.1029/2011GC003649.

Di Stefano, R., Ciaccio, M.G., 2014. The lithosphere and asthenosphere system in Italy as inferred from the Vp and Vs 3D velocity model and Moho map. J. Geodyn. 82, 16-25. http://dx.doi.org/10.1016/j.jog.2014.09.006.

DISS Working Group, 202 . Database of Individual Seismogenic Sources (DISS), Version 3.3.0: A compilation of potential sources for earthquakes larger than M 5.5 in Italy and surrounding areas. Istituto Nazionale di Geofisica e Vulcanologia (INGV). https://doi.org/10.13127/diss3.3.0.

Doglioni, C., 1991. A proposal for the kinematic modelling of W-dipping subductions; possible applications to the Tyrrhenian-Apennines system. Terra Nova 3, 423-434. https://doi.org/10.1111/j.1365-3121.1991.tb00172.x.

Esposito, A., Galvani, A., Sepe, V., Atzori, S., Brandi, G., Cubellis, E., De Martino, P., Dolce, M., Massucci, A., Obrizzo, F., Pietrantonio, G., Riguzzi, F., Tammaro, U., 2020. Concurrent

deformation processes in the Matese massif area (Central-Southern Apennines, Italy). Tectonophysics 774, 228-234. https://doi.org/10.1016/j.tecto.2019.228234.

Faccenna, C., Becker, T.W., Lucente, F.P., Jolivet, L., Rossetti, F., 2001. History of subduction and back-arc extension in the Central Mediterranean. Geophys. J. Int. 145, 809-820. https://doi.org/10.1046/j.0956-540x.2001.01435.x.

Faccenna, C., Civetta, L., D'Antonio, M., Funiciello, F., Margheriti, L., Piromallo, C., 2005. Constraints on mantle circulation around the deforming Calabrian slab. Geophys. Res. Lett. 32, L06311. https://doi.org/10.1029/2004GL021874.

Faccenna, C., Becker, T.W., Auer, L., Billi, A., Boschi, L., Brun, J.-P., Capitanio, F.A., Funiciello, F., Horvàth, F., Jolivet, L., Piromallo, C., Royden, L., Rossetti, F., Serpelloni, E., 2014. Mantle dynamics in the Mediterranean. Rev. Geophys. 52, 283-332. https://doi.org/10.1002/2013RG000444.

Fantoni, R., Franciosi, R., 2010. Tectono-sedimentary setting of the Po Plain and Adriatic foreland. Rend. Fis. Acc. Lincei 21, S197-S209. http://dx.doi.org/10.1007/s12210-010-0102-4.

Ferranti, L., Oldow, J.S., D'Argenio, B., Catalano, R., Lewis, D., Marsella, E., Avellone, G., Maschio, L., Pappone, G., Pepe, F., Sulli, A., 2008. Active deformation in Southern Italy, Sicily and southern Sardinia from GPS velocities of the Peri-Tyrrhenian Geodetic Array (PTGA). Boll. Soc. Geol. Ital. (Ital. J. Geosci.) 127 (2), 299-316.

Ferranti, L., Palano, M., Cannavò, F., Mazzella, M.E., Oldow, J.S., Gueguen, E., Mattia, M., Monaco, C., 2014. Rates of geodetic deformation across active faults in southern Italy. Tectonophysics 621, 101-122. https://doi.org/10.1016/j.tecto.2014.02.007.

Ferri, F., Ventura, R., Coren, F., Zanolla, C., 2005. Gravity map of Italy and surrounding seas. ISPRA, ENI, OGS, 2009. Cartografia Gravimetrica Digitale d'Italia alla scala 1:250.00.

Filippucci, M., Tallarico, A., Dragoni, M., De Lorenzo, S., 2019. Relationship Between Depth of Seismicity and Heat Flow: The Case of the Gargano Area (Italy). Pure Appl. Geophys. 176, 2383-2394. https://doi.org/10.1007/s00024-019-02107-5.

Fischer, T., Horáleka, J., Hrubcováa, P., Vavryuka, V., Bräuerc, K., Kämpfd, H., 2014. Intra-continental earthquake swarms in West-Bohemia and Vogtland: A review. Tectonophysics 611, 1-27. http://dx.doi.org/10.1016/j.tecto.2013.11.001.

Frepoli, A., Marra, F., Maggi, C., Marchetti, A., Nardi, A., Pagliuca, N.M., Pirro, M., 2010. Seismicity, seismogenic structures, and crustal stress fields in the greater Rome area (central Italy). J. Geophys. Res. 115, B12303. http://dx.doi.org/10.1029/2009JB006322.

Frezzotti, M.L., Peccerillo, A., Panza, G., 2009. Carbonate metasomatism and CO_2 lithosphere–asthenosphere degassing beneath the Western Mediterranean: An integrated model arising from petrological and geophysical data. Chem Geol. 262, 108-120. https://doi.org/10.1016/j.chemgeo.2009.02.015.

Galadini, F., 1999. Pleistocene changes in the central Apennine fault kinematics: a key to decipher active tectonics in central Italy. Tectonics 18, 877-894. https://doi.org/10.1029/1999TC900020

Galadini, F., Galli, P., 2000. Active tectonics in the central Apennines (Italy) - input data for seismic hazard assessment. Natural Hazards 22 (3), 225-268. https://doi.org/10.1023/A:1008149531980.

Galvani, A., Anzidei, M., Devoti, R., Esposito, A., Pietrantonio, G., Pisani, A.R., Riguzzi, F., Serpelloni, E., 2012. The interseismic velocity field of the Central Apennine from a dense GPS network. Ann. Geophys. 55, 1039-1049, https://doi.org/10.4401/ag-5634.

Gattaceca, J., Speranza F., 2002. Paleomagnetism of Jurassic to Miocene sediments from the Apenninic carbonate platform (southernApennines, Italy): evidence for a 60° counterclockwise Miocene rotation. Earth Planet. Sci. Lett. 201, 19-34. https://doi.org/10.1016/S0012-821X(02)00686-6.

GeoDAF: Geodetic Data Archiving Facility. http://geodaf.mt.asi.it (accessed 24 March 2022).

Ghisetti, F., Vezzani, L., 2002. Normal faulting, transcrustal permeability and seismogenesis in the Apennines (Italy). Tectonophysics 348 (1-3), 155-168. https://doi.org/10.1016/S0040-1951(01)00254-2.

Giacomuzzi, G., Chiarabba, C., De Gori, P., 2011. Linking the Alps and Apennines subduction systems: New constraints revealed by high-resolution teleseismic tomography. Earth Planet. Sci. Lett. 301 (3-4), 531-543. https://doi.org/10.1016/j.epsl.2010.11.033.

Giacomuzzi, G., Civalleri, M., De Gori, P., Chiarabba, C., 2012. A 3D Vs model of the upper mantle beneath Italy: Insight on the geodynamics of central Mediterranean. Earth Planet. Sci. Lett. 335, 105-120. https://doi.org/10.1016/j.epsl.2012.05.004.

Gischig, V., Gischig, S., Giardini, D., Amann, F., Hertrich, M., Krietsch, H., Loew, S., Maurer, H., Villiger, L., Wiemer, S., Bethmann, F., Brixel, B., Doetsch, J., Doonechaly, N.G., Driesner, T., Dutler, N., Evans, K.F., Jalali, M., Jordan, D., Kittilä, A., Ma, X., Meier, P., Nejati, M., Obermann, A., Plenkers, K., Saar, M.O., Shakas, A., Valley, B., 2020. Hydraulic stimulation and fluid circulation experiments in underground laboratories: Stepping up the scale towards engineered geothermal systems. Geomech. Energy Environ. 24, 100175. https://doi.org/10.1016/j.gete.2019.100175.

Giuliani, R., D'Agostino, N., D'Anastasio, E., Mattone, M., Bonci, L., Calcaterra, S., Gambino, P., Merli, K., 2009. Active crustal extension and strain accumulation from GPS data in the Molise region (central-southern Apennines, Italy). Boll. Geofis. Teor. Appl. 50, 2, 145–156.

Global Volcanism Program, 2013. Volcanoes of the World, v. 4.10.5. Venzke, E. (Ed.). Smithsonian Institution. https://doi.org/10.5479/si.GVP.VOTW4-2013. (accessed 24 March 2022).

Goes, S., Giardini, D., Jenny, S., Hollenstein, C., Kahle, H.-G., Geiger, A., 2004. A recent reorganization in the south-central Mediterranean. Earth Planet. Sci. Lett. 226, 335-345. https://doi.org/10.1016/j.epsl.2004.07.038.

Gold, T., Soter, S., 1984. Fluid ascent through the solid lithosphere and its relation to earthquakes. Pure Appl. Geophys. 122 (2), 492-530. https://doi.org/10.1007/BF00874614.

Govoni, A., Marchetti, A., De Gori, P., Di Bona, M., Lucente, F.P., Improta, L., Chiarabba, C., Nardi, A., Margheriti, L., Piana Agostinetti, N., Di Giovambattista, R., Latorre, D., Anselmi, M., Ciaccio, M.G., Moretti, M., Castellano, C., Piccinini, D., 2014. The 2012 Emilia seismic sequence (Northern Italy): Imaging the thrust fault system by accurate aftershock location. Tectonophysics 622, 44-55. https://doi.org/10.1016/j.tecto.2014.02.013.

Grigoli, F., Cesca, S., Rinaldi, A.P., Manconi, A., López-Comino, J.A., Clinton, J.F., Westaway, R., Cauzzi, C., Dahm, T., Wiemer, S., 2018. The November 2017 Mw5.5 Pohang earthquake: A possible case of induced seismicity in South Korea. Science 360 (6392), 1003-1006. https://doi.org/10.1126/science.aat2010.

Gunatilake, T., Miller, S. A., 2022. Spatio-temporal complexity of aftershocks in the Apennines controlled by permeability dynamics and decarbonization. J. Geophys. Res. 127 (6), e2022JB024154, https://doi.org/10.1029/2022JB024154.

Hainzl, S., 2003. Self-organization of earthquake swarms. J. Geodyn. 35 (1-2), 157-172. https://doi.org/10.1016/S0264-3707(02)00060-1.

Healy, J.H., Rubey, W.W., Griggs, D.T., Raleigh, C.B., 1968. The Denver Earthquakes. Disposal of waste fluids by injection into a deep well has triggered earthquakes near Denver, Colorado. Science 161 (3848), 1301-1310.

Herring, T.A., King, R.W., Floyd, M.A., McClusky, S.C., 2018. Introduction to GAMIT/GLOBK, Release 10.7: GAMIT/GLOBK Documentation. Massachusetts Institute of Technology: Cambridge, UK. http://www-gpsg.mit.edu/.

Herrmann, R.B., Malagnini, L., Munafo, I., 2011. Regional moment tensors of the 2009 L'Aquila earthquake sequence. Bull. Seism. Soc. Am. 101, 975-993. http://dx.doi.org/10.1785/0120100184.

Hubbert, M.K., Rubey, W.W., 1959. Role of fluid pressure in mechanics of overthrust faulting: I. Mechanics of fluid-filled porous solids and its application to overthrust faulting. GSA Bull. 70 (2), 115-166. https://doi.org/10.1130/0016-7606(1959)70[115:ROFPIM]2.0.CO;2.

Hunstad, I., Selvaggi, G., D'Agostino, N., England, P., Clarke, P., Pierozzi, M., 2003. Geodetic strain in peninsular Italy between 1875 and 2001. Geophys. Res. Lett. 30 (4), 1181. http://dx.doi.org/10.1029/2002GL016447.

Hurtig, E., 1991. Geothermal atlas of Europe. International Association of Seismology and Physics of the Earth's Interior. International Heat Flow Commission. Gotha: Hermann Haack Verlagsgesellschaft Geographisch-Kartographische Anstalt.

Hyppolite, J.C., Angelier, J., Roure, F., 1994. A major geodynamic change revealed by quaternary stress patterns in the Southern Apennines (Italy). Tectonophysics 230, 199-210. https://doi.org/10.1016/0040-1951(94)90135-X.

Improta, L., De Gori, P., Chiarabba, C., 2014. New insights into crustal structure, Cenozoic magmatism, CO_2 degassing, and seismogenesis in the southern Apennines and Irpinia region from local earthquake tomography. J. Geophys. Res. 119, 8283-8311. https://doi:10.1002/2013JB010890.

Improta, L., Bagh, S., De Gori, P., Valoroso, L., Pastori, M., Piccinini, D., Chiarabba, C., Anselmi, M., Buttinelli, M., 2017. Reservoir Structure and Wastewater-Induced Seismicity at the Val d'Agri Oilfield (Italy) Shown by Three-Dimensional Vp and Vp/Vs Local Earthquake Tomography. J. Geophys. Res. 122 (11), 9050-9082. https://doi.org/10.1002/2017JB014725.

Irwin, W.P., Barnes, I., 1980. Tectonic relations of carbon dioxide discharges and earthquakes. J. Geophys. Res.: Solid Earth 85 (B6), 3115-3121. https://doi.org/10.1029/JB085iB06p03115.

ISIDe Working Group, 2007. Italian Seismological Instrumental and Parametric Database (ISIDe). Istituto Nazionale di Geofisica e Vulcanologia (INGV). https://doi.org/10.13127/ISIDE (accessed 24 March 2022).

Italiano, F., Martelli, M., Martinelli, G., Nuccio, P.M., 2000. Geochemical evidence of melt intrusions along lithospheric faults of the Southern Apennines, Italy: Geodynamic and seismogenic implications. J. Geophys. Res. 105 (B6), 13569-13578. https://doi.org/10.1029/2000JB900047.

Jenny, S., Goes, S., Giardini, D., Kahle, H.G., 2006. Seismic potential of southern Italy. Tectonophysics 415, 81-101. https://doi.org/10.1016/j.tecto.2005.12.003.

Keranen, K.M., Weingarten, M., Abers, G.A., Bekins, B.A., Ge, S., 2014. Sharp increase in central Oklahoma seismicity since 2008 induced by massive wastewater injection. Science 345 (6195), 448-451. https://doi.org/10.1126/science.1255802.

Keranen, K.M., Weingarten, M., 2018. Induced Seismicity. Annu. Rev. Earth Planet. Sci. 46 (1), 149-174. https://doi.org/10.1146/annurev-earth-082517-010054.

Lee, H., Muirhead, J.D., Fischer, T.P., Ebinger, C.J., Kattenhorn, S.A., Sharp, Z. D., Kianji, G., 2016. Massive and prolonged deep carbon emissions associated with continental rifting. Nat. Geosci. 9, 145-149. https://doi.org/10.1038/ngeo2622.

Louvari, E., Kiratzi, A., Papazachos, B., Hatzidimitriou, P., 2001. Fault-plane solutions determined by waveform modeling confirm tectonic collision in the eastern Adriatic. Pure Appl. Geophys. 158, 1613-1637. https://doi.org/10.1007/PL00001236.

Lucente, F.P., Chiarabba, C., Cimini, G.B., Giardini, D., 1999. Tomographic constraints on the geodynamic evolution of the Italian region. J. Geophys. Res. 104 (B9), 20307-20327. https://doi.org/10.1029/1999JB900147.

Lucente, F.P., De Gori, P., Margheriti, L., Piccinini, D., Di Bona, M., Chiarabba, C., Piana Agostinetti, N., 2010. Temporal variation of seismic velocity and anisotropy before the 2009 Mw 6.3 L'Aquila earthquake, Italy. Geology 38 (11), 1015-1018. https://doi.org/10.1130/G31463.1.

Lupton, J.E., 1983. Terrestrial inert gases: Isotope tracer studies and clues to primordial components in the mantle. Annu. Rev. Earth Planet. Sci. 11, 371-414. https://doi.org/10.1146/annurev.ea.11.050183.002103.

Magnoni, F. Casarotti, E., Komatitsch, D., Di Stefano, R., Ciaccio, M.G., Tape, C., Melini, D., Michelini, A., Piersanti, A., Tromp, J., 2022. Adjoint Tomography of the Italian Lithosphere. Commun Earth Environ 3, 69. https://doi.org/10.1038/s43247-022-00397-7.

Malagnini, L., Lucente, F.P., De Gori, P., Akinci, A., Munafò, I., 2012. Control of pore fluid pressure diffusion on fault failure mode: Insights from the 2009 L'Aquila seismic sequence. Geophys. Res. Lett. 117, B05302. https://doi.org/10.1029/2011JB008911.

Malinverno, A., Ryan, W.B.F., 1986. Extension in the Tyrrhenian Sea and shortening in the Apennines as result of arc migration driven by sinking of the lithosphere. Tectonics 5, 227-245. https://doi.org/10.1029/TC005i002p00227.

Mangiacapra, A., Moretti, R., Rutherford, M., Civetta, L., Orsi, G., Papale, P., 2008. The deep magmatic system of the Campi Flegrei caldera (Italy). Geophys. Res. Lett. 35, L21304. https://doi:10.1029/2008GL035550.

Manu-Marfo, D., Aoudia, A., Pachhai, S., Kherchouche, R., 2019. 3D shear wave velocity model of the crust and uppermost mantle beneath the Tyrrhenian basin and margins. Sci. Rep. 9 (1), 1-10. https://doi.org/10.1038/s41598-019-40510-z.

Marani, M., Trua, T., 2002. Thermal constriction and Tera faulting at the origin of a super-inflated spreading centre: the Marsili volcano, Tyrrhenian Sea. J. Geophys. Res. Solid Earth 107 (B9), 2188. https://doi.org/10.1029/2001JB000285.

Mariucci, M.T., Montone, P., 2020. Database of Italian present-day stress indicators, IPSI 1.4. Sci. Data 7, 298. https://doi.org/10.1038/s41597-020-00640-w.

Marroni, M., Meneghini, F., Pandolfi, L., 2010. Anatomy of the Ligure-Piemontese subduction system. Int. Geol. Rev. 52 (10-12), 1160-1192. https://doi.org/10.1080/00206810903545493.

Martelli, M., Nuccio, P.M., Stuart, F.M., Burgess, R., Ellam, R.M., Italiano, F., 2004. Helium-strontium isotope constraints on mantle evolution beneath the Roman Comagmatic Province, Italy. Earth Planet. Sci. Lett. 224 (3-4), 295-308. https://doi.org/10.1016/j.epsl.2004.05.025.

Márton, E., 2003. Palaeomagnetic evidence for tertiary counterclockwise rotation of Adria. Tectonophysics 377 (1-2), 143-156. https://doi.org/10.1016/j.tecto.2003.08.022.

Márton, E., Ćosović, V., Moro, A., Zvocak, S., 2008. The motion of Adria during the late Jurassic and Cretaceous: New paleomagnetic results from stable Istria. Tectonophysics 454, 44-53. https://doi.org/10.1016/j.tecto.2008.04.002.

Massin, F., Farrell, J., Smith, R.B., 2013. Repeating earthquakes in the Yellowstone volcanic field: Implications for rupture dynamics, ground deformation, and migration in earthquake swarms. J. Volcanol. Geoth. Res. 257, 159-173. https://doi.org/10.1016/j.jvolgeores.2013.03.022.

Mazzoli, S., D'Errico, M., Aldega, L., Corrado, S., Invernizzi, C., Shiner, P., Zattin, M., 2008. Tectonic burial and 'young' (<10 Ma) exhumation in the southern Apennines fold and thrust belt (Italy), Geology 36, 243-246. https://doi.org/10.1130/G24344A.1.

McKinstry, H.E., 1948. Mining geology. New York, Prentice-Hall.

Métois, M., D'Agostino, N., Avallone, A., Chamot-Rooke, N., Rabaute, A., Duni, L., Kuka, N., Koci, R., Georgiev, I., 2015. Insights on continental collisional processes from GPS data: Dynamics of the peri-Adriatic belts. J. Geophys. Res. 120, 8701-8719. https://doi:10.1002/2015JB012023.

Milia, A., Torrente, M. M., Russo, M., Zuppetta A., 2003. Tectonics and crustal structure of the Campania continental margin: relationships with volcanism. Mineral. Petrol. 79, 33-47. https://doi.org/10.1007/s00710-003-0005-5.

Miller, S.A., Collettini, C., Chiaraluce, L., Cocco, M., Barchi, M., Kaus, B.J.P., 2004. Aftershocks driven by a high-pressure CO_2 source at depth. Nature 427, 724-727. https://doi.org/10.1038/nature02251.

Miller, S., 2013. The role of fluids in tectonic and earthquake processes. Adv. Geophys. 54, 1-46. https://doi.org/10.1016/B978-0-12-380940-7.00001-9.

Minissale, A., 2004. Origin, transport and discharge of CO_2 in central Italy. Earth-Sci. Rev. 66 (1-2), 89-141. https://doi.org/10.1016/j.earscirev.2003.09.001.

Minissale, A., Donato, A., Procesi, M., Pizzino, L., Giammarco, S., 2019. Systematic review of geochemical data from thermal springs, gas vents and fumaroles of Southern Italy for geothermal favourability mapping. Earth-Sci. Rev. 188, 514-535. https://doi.org/10.1016/j.earscirev.2018.09.008.

Molinari, I., Morelli, A., 2011. EPcrust: a reference crustal model for the European Plate. Geophys. J. Int. 185 (1), 352-364. https://doi.org/10.1111/j.1365-246X.2011.04940.x.

Molinari, I., Verbeke, J., Boschi, L., Kissling, E., Morelli, A., 2015. Italian and Alpine three dimensional crustal structure imaged by ambient-noise surface-wave dispersion. Geochem. Geophys. Geosys. 16 (12), 4405-4421. https://doi.org/10.1002/2015GC006176.

Molli, G., 2008. Northern Apennine-Corsica orogenic system: an updated overview. Geological Society, London, Special Publications 298 (1), 413-442. https://doi.org/10.1144/SP298.19.

Moment Tensor Details for Italy, 2008. http://www.eas.slu.edu/eqc/eqc_mt/MECH.IT/ (accessed 24 March 2022).

Mongelli, F., Zito, G., Vedova, B.D., Pellis, G., Squarci, P., Taffi, L., 1991. Geothermal regime of Italy and surrounding seas, in: Čermák, V., Rybach, L. (Eds.), Terrestrial Heat Flow and the Lithosphere Structure. Exploration of the Deep Continental Crust. Springer, Berlin, Heidelberg pp. 381-394. https://doi.org/10.1007/978-3-642-75582-8_18.

Mousavi, S., Bauer, K., Korn, M., Hejrani, B., 2015. Seismic tomography reveals a mid-crustal intrusive body, fluid pathways and their relation to the earthquake swarms in West Bohemia/Vogtland. Geophys. J. Int. 203 (2), 1113-1127. https://doi.org/10.1093/gji/ggv338.

Napolitano, F., De Siena, L., Gervasi, A., Guerra, I., Scarpa, R., La Rocca, M., 2020. Scattering and absorption imaging of a highly fractured fluid-filled seismogenetic volume in a region of slow deformation. Geosci. Front. 11 (3), 989-998. https://doi.org/10.1016/j.gsf.2019.09.014.

Nicolosi, I., Speranza, F., Chiappini, M., 2006. Ultrafast oceanic spreading of the Marsili basin, southern Tyrrhenian Sea: Evidence from magnetic anomaly analysis. Geology 34(9), 717-720. https://doi.org/10.1130/G22555.1.

Palano, M., Cannavò, F., Ferranti, L., Mattia, M., Mazzella, M.E., 2011. Strain and stress fields in the southern Apennines (Italy) constrained by geodetic, seismological and borehole data. Geophys. J. Int. 187 (3), 1270-1282. https://doi.org/10.1111/j.1365-246x.2011.05234.x.

Palano, M., Pezzo, G., Serpelloni, E., Devoti, R., D'Agostino, N., Gandolfi, S., Sparacino, F., Anderlini, L., Poluzzi, L., Tavasci, L., Macini, P., Pierantonio, G., Riguzzi, F., Antoncecchi, I., Ciccone, F., Rossi, G., Avallone, A., Selvaggi, G. 2020. Geopositioning time series from offshore platforms in the Adriatic Sea. Sci. Data 7, 373. https://doi.org/10.1038/s41597-020-00705-w.

Patacca, E., Scandone, P., 1989. Post-Tortonian mountain building in the Apennines. The role of the passive sinking of a relic lithospheric slab, in: Boriani, A., Bonafede, M., Piccardo, G.B. Vai, G.B. (Eds.), The Lithosphere in Italy: Advances in Earth Science Research 80, pp. 157-176, Accademia Nazionale dei Lincei, Rome.

Patacca, E., Sartori, R., Scandone, P., 1990. Tyrrhenian basin and Appeninic Arcs: kinematic relations since late Tortonian times. Mem. Soc. Geol. It. 45, 425-451.

Patacca, E., Scandone, P., 2001. Late thrust propagation and sedimentary response in the thrust belt-foredeep system of the southern Apennines (Pliocene-Pleistocene), in: Vai, G.B., Martini, I.P. (Eds.), Anatomy of a Mountain: The Apennines and Adjacent Mediterranean Basins. Kluwer Acad., Dordrecht, Netherlands, pp. 401-440. https://doi.org/10.1007/978-94-015-9829-3_23.

Patacca, E., Scandone, P., 2007. Geological interpretation of the CROP-04 seismic line (southern Apennines, Italy). Boll. Soc. Geol. Ital. (Ital. J. Geosci.) 7, 297-315.

Patacca, E., Scandone, P., Di Luzio, E., Cavinato, G.P., Parotto, M., 2008. Structural architecture of the central Apennines: Interpretation of the CROP 11 seismic profile from the Adriatic coast to the orographic divide. Tectonics 27, TC3006, 1-36. https://doi.org/10.1029/2005TC001917.

Peccerillo, A., Lustrino, M., 2005. Compositional variations of Plio-Quaternary magmatism in the circum-Tyrrhenian area: Deep versus shallow mantle processes. (Eds.) Gillian R. Foulger, James H. Natland, Dean C. Presnall, Don L. Anderson. Plates, plumes and paradigms. Geolog. Soc. Am. 388. https://doi.org/10.1130/SPE388.

Pezzo, G., De Gori, P., Lucente, F.P., Chiarabba, C., 2018. Pore pressure pulse drove the 2012 Emilia (Italy) series of earthquakes. Geophys. Res. Lett. 45 (2), 682-690. https://doi.org/10.1002/2017GL076110 .

Piana Agostinetti, N., Amato, A., 2009. Moho depth and Vp/Vs ratio in peninsular Italy from teleseismic receiver functions. J. Geophys. Res. 114, B06303. https://doi.org/10.1029/2008JB005399.

Piccardi, L., Tondi, G., Cello, G., 2006. Geo-structural evidence for active oblique extension in South-Central Italy. In: Pinter, N., Gyula, G., Weber, J., Stein, S., Medak, D. (Eds.), The Adria microplate: GPS Geodesy, Tectonics and Hazard. Nato Science Series: IV: Earth and Environmental Sciences 61, Springer, Dordrecht. https://doi.org/10.1007/1-4020-4235-3_07.

Piccinini, D., Saccorotti, G., 2008. First observations of non-volcanic, long-period seismicity in the central Apennines, Italy. Geophys. Res. Lett. 35, L12303. https://doi.org/10.1029/2008GL034120.

Pino, N.A., Di Luccio, F., 2005. Seismic recording of small zero frequency displacement from moderate events. Geophys. Res. Lett. 32, L12304. https://doi.org/10.1029/2005GL022780.

Piromallo, C., Morelli, A., 2003. P wave tomography of the mantle under the Alpine-Mediterranean area. J. Geophys. Res. 108, 2065. https://doi.org/10.1029/2002JB001757.

Pondrelli, S., 1999. Pattern of seismic deformation in the Western Mediterranean. Ann. Geophys. 42 (1). https://doi.org/10.4401/ag-3700.

Pondrelli, S., Salimbeni, S., Ekström, G., Morelli, A., Gasperini, P., Vannucci, G., 2006. The Italian CMT dataset from 1977 to the present. Phys. Earth Planet. Inter. 159, 286-303. https://doi.org/10.1016/j.pepi.2006.07.008.

Raleigh, C.B., Healy, J. H., Bredehoeft, J.D., 1976. An Experiment in Earthquake Control at Rangely, Colorado. Science 191, 1230-1237.

Rosenbaum, G., Lister, G. S., 2004. Neogene and Quaternary rollback evolution of the Tyrrhenian Sea, the Apennines and the Sicilian Maghrebides. Tectonics, 23, TC1013, https://doi.org/10.1029/2003TC001518.

Rosenbaum, G., Lister, G. S., Douboz, C., 2004. Mesozoic and Cenozoic motion of Adria (central Mediterranean): A review of constraints and limitations. Geodinamica Acta 17, 125-139. https://doi.org/10.3166/ga.17.125-139

Rovida, A., Locati, M., Camassi, R., Lolli, B., Gasperini, P., Antonucci, A., 2022. Catalogo Parametrico dei Terremoti Italiani (CPTI15), versione 4.0. Istituto Nazionale di Geofisica e Vulcanologia (INGV). https://doi.org/10.13127/CPTI/CPTI15.4.

Satolli, S., Speranza, F., Calamita, F., 2005. Paleomagnetism of the Gran Sasso range salient (Central Apennines, Italy): pattern of orogenic rotations due to translation of a massive carbonate indenter. Tectonics 24, TC4019. https://doi.org/10.1029/2004TC001771.

Scognamiglio, L., Magnoni, F., Tinti E., Casarotti E., 2016. Uncertainty estimations for moment tensor inversions: the issue of the 2012 May 20 Emilia earthquake. Geophys. J. Int. 206 (2), 792-806. https://doi.org/10.1093/gji/ggw173.

Scognamiglio, L., Tinti, E., Quintiliani, M., 2006. Time Domain Moment Tensor (TDMT). Istituto Nazionale di Geofisica e Vulcanologia (INGV). https://doi.org/10.13127/tdmt.

Sebastiani, G., Govoni, A., Pizzino, L., 2019. Aftershock patterns in recent central Apennines sequences. J. Geophys. Res. 124. https://doi.org/10.1029/2018JB017144.

Selvaggi, G., Amato, A., 1992. Intermediate depth earthquakes in the Northern Apennines (Italy): evidence for a still active subduction? Geophys. Res. Lett. 19, 2127-2130.

Selvaggi, G., Chiarabba, C., 1995. Seismicity and P-wave velocity image of the Southern Tyrrhenian subduction zone. Geophys. J. Int. 121, 818-826. https://doi.org/10.1111/j.1365-246X.1995.tb06441.x.

Serpelloni, E., Faccenna, C., Spada, G., Dong, D., Williams, S.D., 2013. Vertical GPS ground motion rates in the Euro-Mediterranean region: New evidence of velocity gradients at different spatial scales along the Nubia-Eurasia plate boundary. J. Geophys. Res. 118 (11), 6003-6024. https://doi.org/10.1002/2013JB010102

Shapiro, S.A., Dinske, C., 2009. Fluid-induced seismicity: Pressure diffusion and hydraulic fracturing. Geophys. Prospect. 57, 301-310. https://doi.org/10.1111/j.1365-2478.2008.00770.x

Shen, Z.-K., Wang, M., Zeng, Y., Wang, F., 2015. Optimal interpolation of spatially discretized geodetic data. Bull. Seismol. Soc. Am. 105, 2117-2127. https://doi:10.1785/0120140247.

Sibson, R.H., 1992. Implications of fault-valve behaviour for rupture nucleation and recurrence. Tectonophysics 211 (1-4), 283-293. https://doi.org/10.1016/0040-1951(92)90065-E.

Sibson, R.H., 2020. Preparation zones for large crustal earthquakes consequent on fault-valve action. Earth Planets Space 72, 31. https://doi.org/10.1186/s40623-020-01153-x.

Simpson, D.W., 1986. Triggered earthquakes. Ann. Rev. Earth Planet. Sci. 14, 21-42.

Smith-Konter, B.R., Sandwell, D.T., Shearer, P., 2011. Locking depths estimated from geodesy and seismology along the San Andreas Fault System: Implications for seismic moment release. J. Geophys. Res. 116, B06401. https://doi.org/10.1029/2010JB008117.

Spada, M., Bianchi, I., Kissling, E., Agostinetti, N.P., Wiemer, S., 2013. Combining controlled-source seismology and receiver function information to derive 3-D Moho topography for Italy. Geophys. J. Int. 194, 1050-1068. https://doi.org/10.1093/gji/ggt148.

Speranza, F., 2003. Genesis and evolution of a curved mountain front: paleomagnetic and geological evidence from the Gran Sasso range (Central Apennines, Italy). Tectonophysics 362, 183-197. https://doi.org/10.1016/S0040-1951(02)00637-6.

Tamburello, G., Pondrelli, S., Chiodini, G., Rouwet, D., 2018. Global-scale control of extensional tectonics on CO_2 earth degassing. Nat. Commun. 9, 4608. https://doi.org/10.1038/s41467-018-07087-z.

Terakawa, T., Zoporowski, A., Galvan, B., Miller, S.A., 2010. High-pressure fluid at hypocentral depths in the L'Aquila region inferred from earthquake focal mechanisms. Geology 38 (11), 995-998. https://doi.org/10.1130/G31457.1.

Totaro, C., Koulakov, I., Orecchio, B., Presti, D., 2014. Detailed crustal structure in the area of the southern Apennines–Calabrian Arc border from local earthquake tomography. J. Geodyn. 82, 87-97. https://doi.org/10.1016/j.jog.2014.07.004.

Trasatti, E., Marra, F., Polcari, M., Stiope, G., Ciotoli, G., Darrah, T., Tedesco, D., Stramondo, S., Florindo, F., Ventura, G., 2018. Coeval uplift and subsidence reveal magma recharging near Rome, Geochemistry, Geophysics, Geosystems 19, 1484-1498. https://doi.org/10.1029/2017GC007303.

Vallée, M., Di Luccio, F., 2005. Source analysis of the 2002 Molise, southern Italy, twin earthquakes (10/31 and 11/01). Geophys. Res. Lett. 32, L12309. https://doi.org/10.1029/2005GL022687.

van Hinsbergen, D.J.J., Vissers, R.L., Spakman, W., 2014. Origin and consequences of western Mediterranean subduction, rollback, and slab segmentation. Tectonics 33, 393-419. https://doi.org/10.1002/2013TC003349.

Vannoli, P., Martinelli, G., Valensise, G., 2021. The Seismotectonic Significance of Geofluids in Italy. Front. Earth Sci. 9. https://doi.org/10.3389/feart.2021.579390.

Ventura, G., Di Giovambattista, R., 2013. Fluid pressure, stress field and propagation style of coalescing thrusts from the analysis of the 20 May 2012 M_L 5.9 Emilia earthquake (Northern Apennines, Italy). Terra Nova 25 (1), 72-78. https://doi.org/10.1111/ter.12007.

Ventura, G., Cinti, F.R., Di Luccio, F., Pino, N.A., 2007. Mantle wedge dynamics versus crustal seismicity in the Apennines (Italy). Geochem. Geophys. Geosys. 8 (2), Q02013. https://doi.org/10.1029/2006GC001421.

Verbeke, J., Boschi, L., Stehly, L., Kissling, E., Michelini, A., 2012. High-resolution Rayleigh-wave velocity maps of central Europe from a dense ambient-noise data set. Geophys. J. Int. 188 (3), 1173-1187. https://doi.org/10.1111/j.1365-246X.2011.05308.x.

Vezzani, L., Festa, A., Ghisetti, F.C., 2010. Geology and Tectonic Evolution of the Central-Southern Apennines, Italy, in: Geology and Tectonic Evolution of the Central-Southern Apennines, Italy. Geolog. Soc. Am. 469, 1-58. https://doi.org/10.1130/2010.2469.

Viganò, A., Scafidi, D., Martin, S., Spallarossa, D., 2013. Structure and properties of the Adriatic crust in the central-eastern Southern Alps (Italy) from local earthquake tomography. Terra Nova 25 (6), 504-512. https://doi.org/10.1111/ter.12067.

Vitale, S., Ciarcia, S., Tramparulo, F.D.A., 2013. Deformation and stratigraphic evolution of the Ligurian Accretionary Complex in the Southern Apennines (Italy). J. Geodyn. 66, 120-133. https://doi.org/10.1016/j.jog.2013.02.008.

Viti M., Viti E., Babbucci D., Tamburelli C., Cenni N., Baglione M., D'Intinosante V., 2015. Belt-Parallel shortening in the northern Apennines and seismotectonic implications. Int. J. Geosci. 6, 938-961, https://doi.org/10.4236/ijg.2015.68075.

Ward, S.N., 1998. On the consistency of earthquake moment release and space geodetic strain rates: Europe. Geophys. J. Int. 135 (3), 1011-1018. https://doi.org/10.1046/j.1365-246X.1998.t01-2-00658.x.

Wessel, P., Luis, J. F., Uieda, L., Scharroo, R., Wobbe, F., Smith, W. H. F., Tian, D., 2019. The Generic Mapping Tools version 6. Geochem. Geophys. Geosys. 20, 5556-5564. https://doi.org/10.1029/2019GC008515.

Wortel, M.J.R., Spakman, W., 2000. Subduction and slab detachment in the Mediterranean Carpathian region. Science 290, 1910-1917. https://doi.org/10.1126/science.290.5498.1910.

Yoshida, K., Hasegawa, A., 2018. Hypocenter Migration and Seismicity Pattern Change in the Yamagata-Fukushima Border, NE Japan, Caused by Fluid Movement and Pore Pressure Variation. J. Geophys. Res. Solid Earth 123 (6), 5000-5017. https://doi.org/10.1029/2018JB015468.

Zhang, G., Lei, J., Sun, D., 2019. The 2013 and 2017 M$_W$ 3 seismic swarms in Jilin, NE China: Fluid triggered earthquakes? J. Geophys. Res. Solid Earth 124 (12), 13096-13111. https://doi.org/10.1029/2019JB018649.

Zhang, G., Wu, A., Li, H., Qu, H., Li, Y., Xiao, L., Zhang, Z., Shen, J., 2021. Hydrocarbon Enrichment and Main Controlling Factors in Offshore Rift Basins of China: A Case Study in the Beibuwan Basin. Acta Geologica Sinica (English Edition), 95 (1), 192-207. https://doi.org/10.1111/1755-6724.14632.

Zoback, M.D., Townend, J., Grollimund, B., 2002. Steady-State Failure Equilibrium and Deformation of Intraplate Lithosphere. Int. Geol. Rev. 44, 383-401. https://doi.org/10.2747/0020-6814.44.5.383.

FIGURE CAPTIONS

Figure 1. The study area in the framework of the Europe-Africa collision. A) Simplified geological setting of the Mediterranean region. 1) post-orogenic basins, 2) Neogene shortening, 3) Neogene oceanic crust, 4) main thrust faults, 5) strike slip faults, 6) normal faults. B) Spatial distribution of the seismic stations over the Italian region. C) Simplified tectonic setting of the Apennines. Holocene and Pleistocene volcanoes

(https://volcano.si.edu) are reported as brown and red triangles, respectively. Abbreviation are: AH, Albani Hills; Am, Amiata; Ca, Campania; CDS, Campanian degassing structure; CAP, Central Apennines; Ga, Gargano; Is, Ischia; La, Larderello; Lat, Latium; Me, Mefite D'Ansanto; NAP, Northern Apennines; PF, Phlegrean Fields; Po, Pollino Massif; PP, Po Plain; Ro, Roccamonfina volcano; SAP, Southern Apennines; SM, Sannio-Matese; TRDS, Tuscan-Roman degassing structure; Ve, Vesuvius; Vu, Mount Vulture.

Figure 2. Seismological observations. A) (left) Map of the historical seismicity smaller (green) and larger than 6.5 (red). (right) Latitude of the historical seismicity is plotted against magnitude to highlight that the strongest shocks occurred in the southern Apennines. B) Instrumented seismicity (1985-2021, ISIDe Working Group, 2007) larger than 1.5 is color coded with depth. The major seismic sequences occurred since the development of the INGV seismic network are also indicated (from north to south): Em=2012 M_w^{max}5.9 Emilia, UM=1997-1998 M_w^{max}6.0 Umbria-Marche, AN=2016 M_w^{max}6.5 Amatrice-Norcia, Aq=2009 M_w^{max}6.3 L'Aquila, SM=2013-2014 M_w^{max}5 Sannio-Matese, Mo=2002 M_w^{max}5.8 Molise, Pz=1990 M_w^{max}5.7 Potenza, Ir=1980 M_S6.9 Irpinia, Po=2012 M_L^{max}5 Pollino. c) Available moment tensor solutions of earthquakes larger than 4 (https://doi.org/10.13127/TDMT, TDMT, Scognamiglio et al., 2006; http://www.eas.slu.edu/eqc/eqc_mt/MECH.IT/, Herrmann et al., 2011) are colored as a function of rake. d) Maximum horizontal stress field distribution (Mariucci and Montone, 2020).

Figure 3. **Geochemical and geophysical observations.** A) CO_2 flux distribution (Chiodini et al., 2000, 2004). B) Conductive heat flow map (Della Vedova et al., 2001). Crossed black circles represent the sampled aquifers. C) Moho depth from controlled-source seismology and receiver functions (Spada et al., 2013). D) Bouguer anomalies (Ferri et al., 2005).

Figure 4. Geophysical and seismological observations. A) Seismogenic thickness computed in this study. B) GNSS velocity vectors referred to Eurasia overlap the color-shaded background vertical velocity. C) Distribution of the main strain axes (red is dilatation and blue is contraction) is shown above the areal dilatation.

Figure 5. Crustal tomography. A-C) Shear-wave velocity and D-F) Vp/Vs anomalies at crustal depths (Di Stefano and Ciaccio, 2014).

Figure 6. Mantle tomography. A-C) Mantle shear-wave velocity and D-F) Vp/Vs anomalies (Giacomuzzi et al., 2012).

Figure 7. Geochemical and geophysical cross-sections and shear wave tomography. Geochemical and geophysical parameters are plotted in SW-NE profiles that cross the northern (A), central (B) and (C, D, E) southern Apennines, respectively (profile locations are shown in the bottom right panel). In each set of profiles, the following parameters are plotted from top to bottom: topography; the CO_2 (Chiodini et al., 2000, 2004) and the conductive heat flow (Della Vedova et al., 2001) trends as blue and green lines, respectively, and the aquifer locations (Ca) (Chiodini et al., 2000, 2004); GNSS deformation vectors projected along the strike of the profile (black and red for the GNSS stations located within ± 10 and ± 30 km from the profile trace, respectively) and the 2nd invariant of the strain (computed in this study); Mh= the Moho depth as black line (Spada et al., 2013); St=the seismogenic thickness computed in this study as yellow line; the Bouguer anomaly as red line (Ferri et al., 2005); the crustal seismicity from January 1985 to April 2021 with magnitude larger than 1.5 located within ± 25 km from the profile trace (ISIDe Working Group, 2007) as gray dots and histograms (at the bottom of the figure with a bin size of 2.5 km); shear wave velocity anomalies are from Di Stefano and Ciaccio (2014) at crustal depths and from Giacomuzzi et al. (2012) at upper mantle depths. F) SW-NE profiles in map view; abbreviations are as Fig. 1c, Cn, Candelaro.

Figure 8. Geochemical and geophysical cross-sections and Vp/Vs tomography.

Same as in Figure 7, except that here Vp/Vs anomalies are plotted.

CO_2 Earth degassing and geodynamics of the Apennines, Italy

All the authors know and concur with the submission of this manuscript to **Earth-Science Reviews** journal and declare that they have no known competing financial interests or personal relationships that could have appeared to influence the work reported in this paper.

Francesca Di Luccio and Mimmo Palano on behalf of the co-authors

CRediT author statement

F. Di Luccio, M. Palano: Conceptualization, Methodology, Investigation, Resources, Data curation, Formal analysis, Writing - Original Draft, Writing - Review & Editing, Visualization, Supervision. **F. Di Luccio**: Project administration, Funding acquisition. **G. Chiodini, L. Cucci, C. Piromallo, F. Sparacino G. Ventura:** Conceptualization, Methodology, Validation, Investigation, Resources, Data curation, Formal analysis, Writing - Original Draft, Writing - Review & Editing. **L. Improta, C. Cardellini, P. Persaud, L. Pizzino**: Formal analysis, Writing - Review & Editing. **G. Calderoni, C. Castellano, G. Cianchini, S. Cianetti, D. Cinti, P. Cusano, P. De Gori, A. De Santis, P. Del Gaudio, G. Diaferia, A. Esposito, D. Galluzzo, A. Galvani, A. Gasparini, G. Gaudiosi, A. Gervasi, C. Giunchi, M. La Rocca, G. Milano, S. Morabito, L. Nardone, M. Orlando, S. Petrosino, D. Piccinini, G. Pietrantonio, A. Piscini, P. Roselli, D. Sabbagh, A. Sciarra, L. Scognamiglio, V. Sepe, A. Tertulliani, R. Tondi, L. Valoroso, N. Voltattorni, L. Zuccarello:** Writing - Review & Editing.

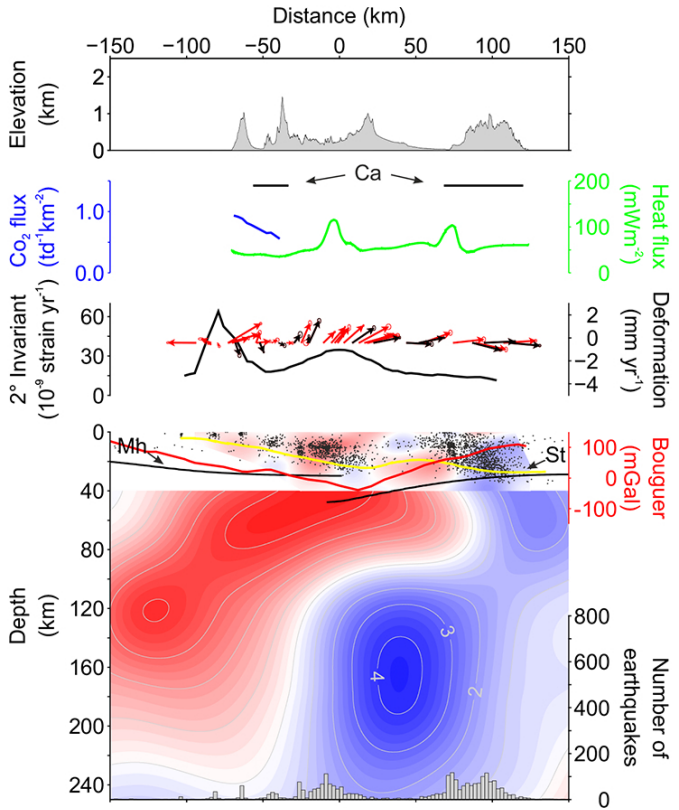

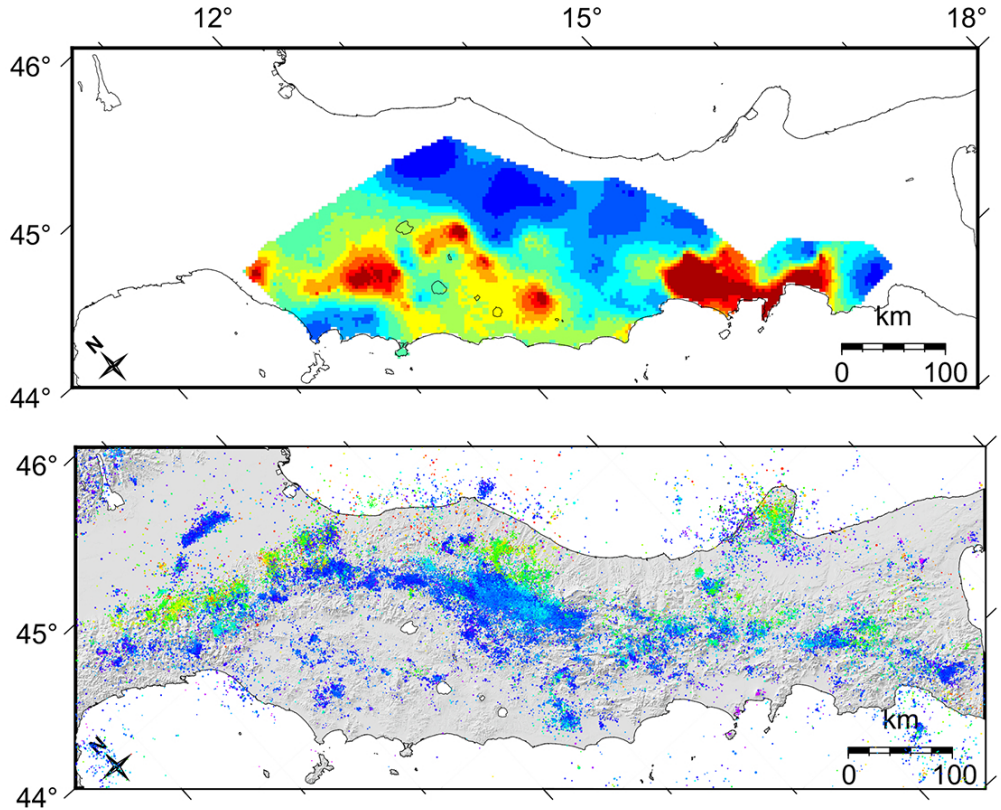

Graphics Abstract

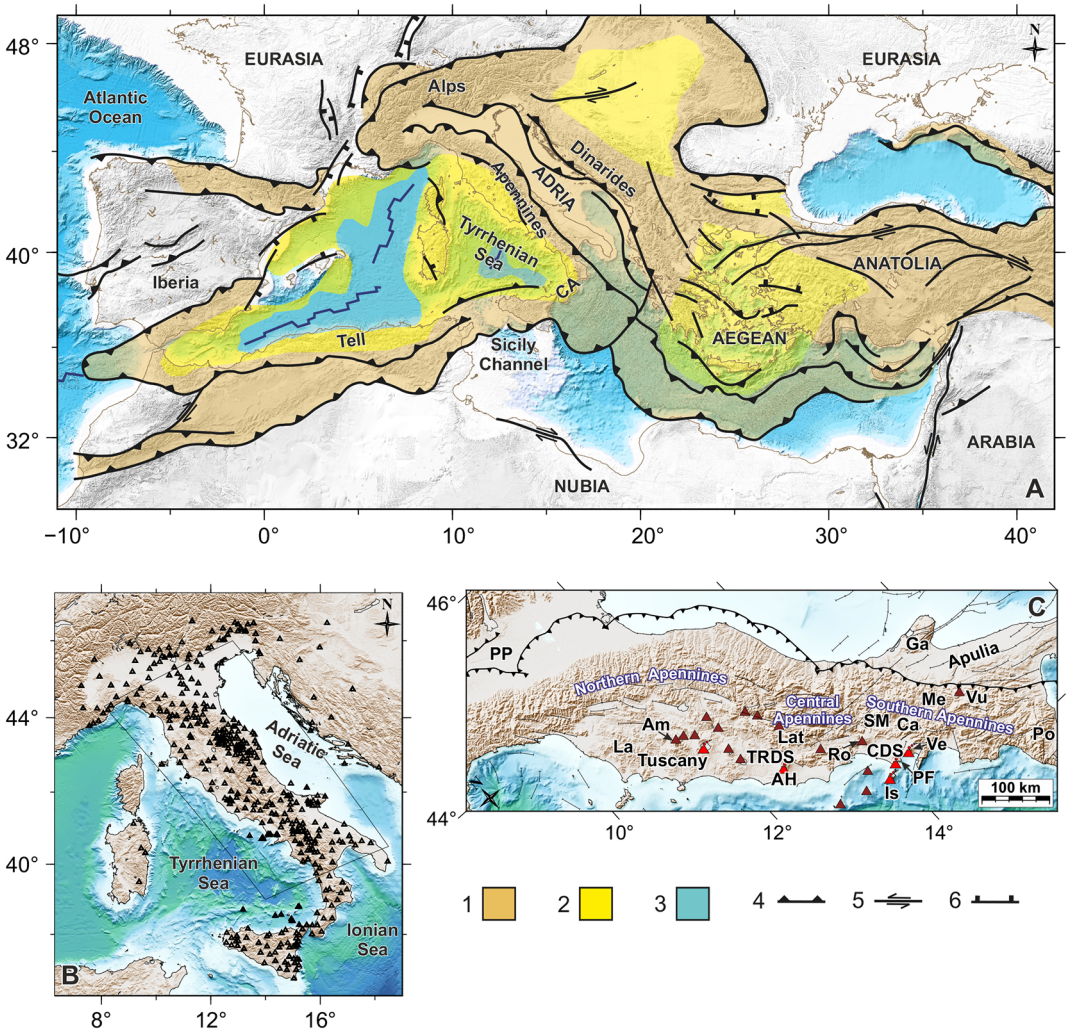
EURASIA
Atlantic Ocean
Alps
Dinarides
ADRIA
Apennines
Tyrrhenian Sea
CA
Iberia
Tell
Sicily Channel
AEGEAN
ANATOLIA
ARABIA
NUBIA
A
48°
40°
32°
−10°
0°
10°
20°
30°
40°
N
B
Adriatic Sea
Tyrrhenian Sea
Ionian Sea
44°
40°
8°
12°
16°
C
PP
Northern Apennines
Central Apennines
Southern Apennines
Apulia
Ga
Me
Vu
Ca
SM
Am
La
Tuscany
Lat
TRDS
Ro
CDS
Ve
Po
AH
PF
Is
100 km
46°
44°
10°
12°
14°
1
2
3
4
5
6

Figure 1

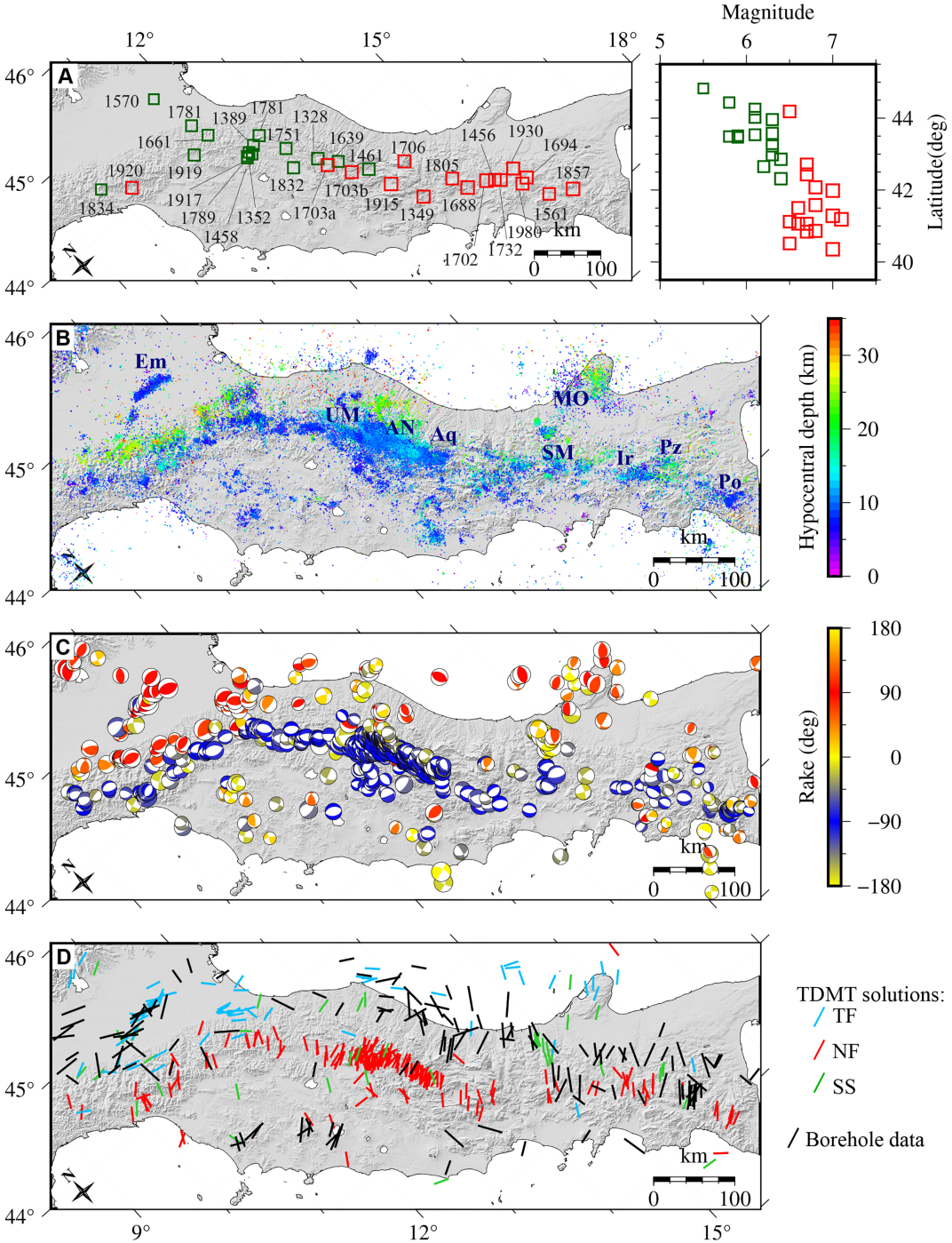
A
B
C
D
12°
15°
18°
46°
45°
44°
9°
Magnitude
5
6
7
Latitude(deg)
44
42
40
1570
1781
1389
1781
1328
1661
1751
1639
1456
1930
1694
1706
1461
1805
1857
1920
1919
1832
1703b
1915
1688
1834
1917
1789
1352
1703a
1349
1561
1458
1980
1732
1702
km
0
100
Em
UM
AN
Aq
MO
SM
Ir
Pz
Po
Hypocentral depth (km)
30
20
10
0
Rake (deg)
180
90
0
−90
−180
TDMT solutions:
TF
NF
SS
Borehole data

Figure 2

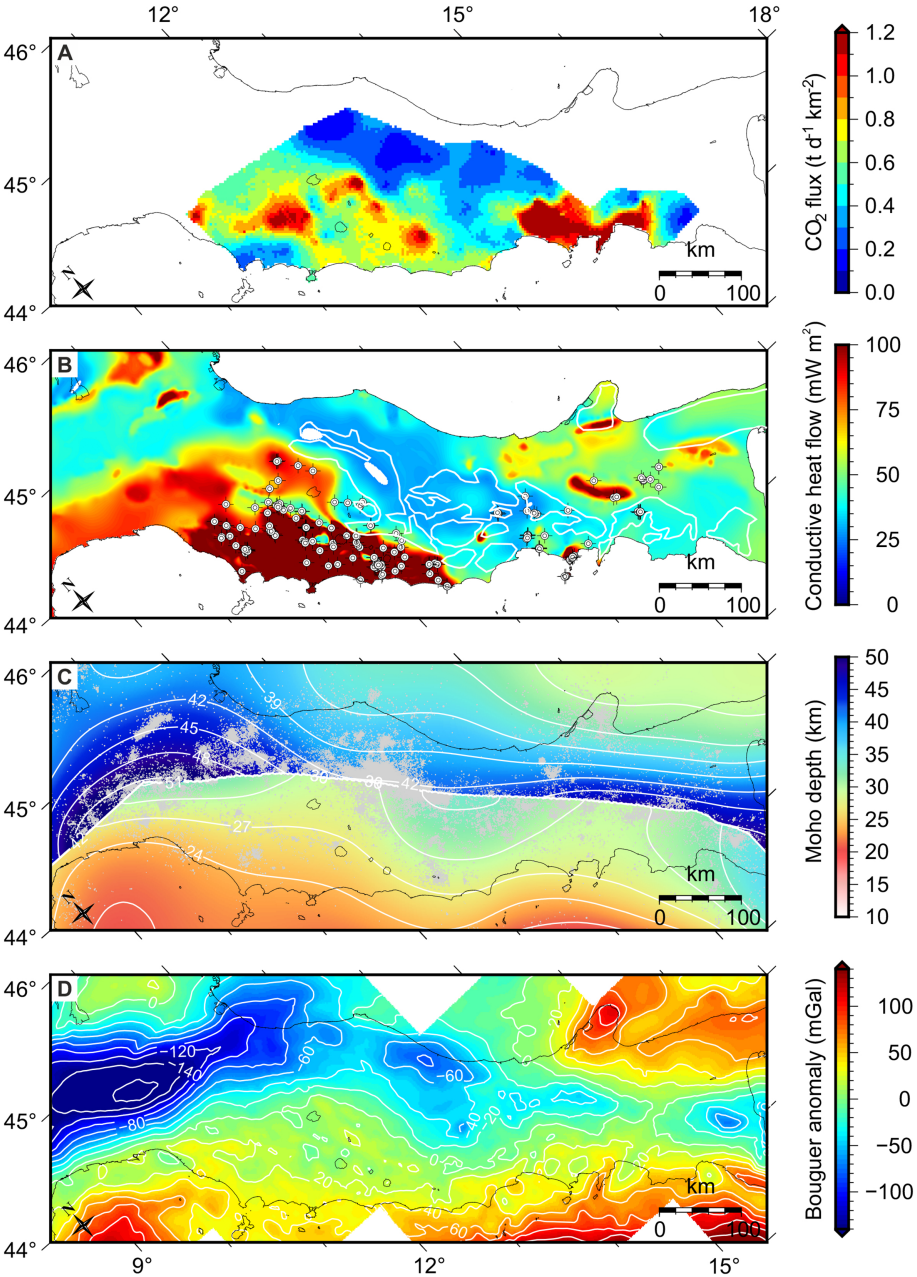
12°
15°
18°
46°
45°
44°
A
km
0
100
CO2 flux (t d-1 km-2)
1.2
1.0
0.8
0.6
0.4
0.2
0.0
B
Conductive heat flow (mW m2)
100
75
50
25
0
C
Moho depth (km)
50
45
40
35
30
25
20
15
10
D
Bouguer anomaly (mGal)
100
50
0
−50
−100
9°

Figure 3

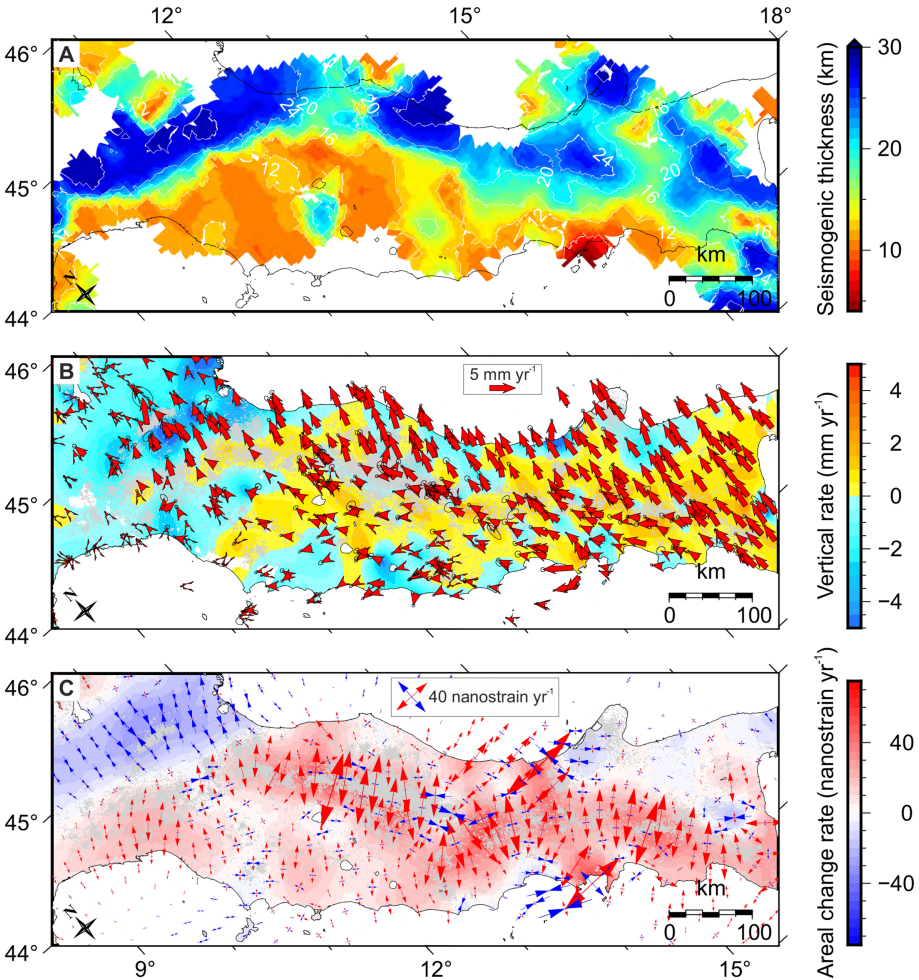
12°
15°
18°
46°
45°
44°
A
B
C
km
0
100
Seismogenic thickness (km)
30
20
10
5 mm yr-1
Vertical rate (mm yr-1)
4
2
0
−2
−4
40 nanostrain yr-1
Areal change rate (nanostrain yr-1)
40
0
−40
9°

Figure 4

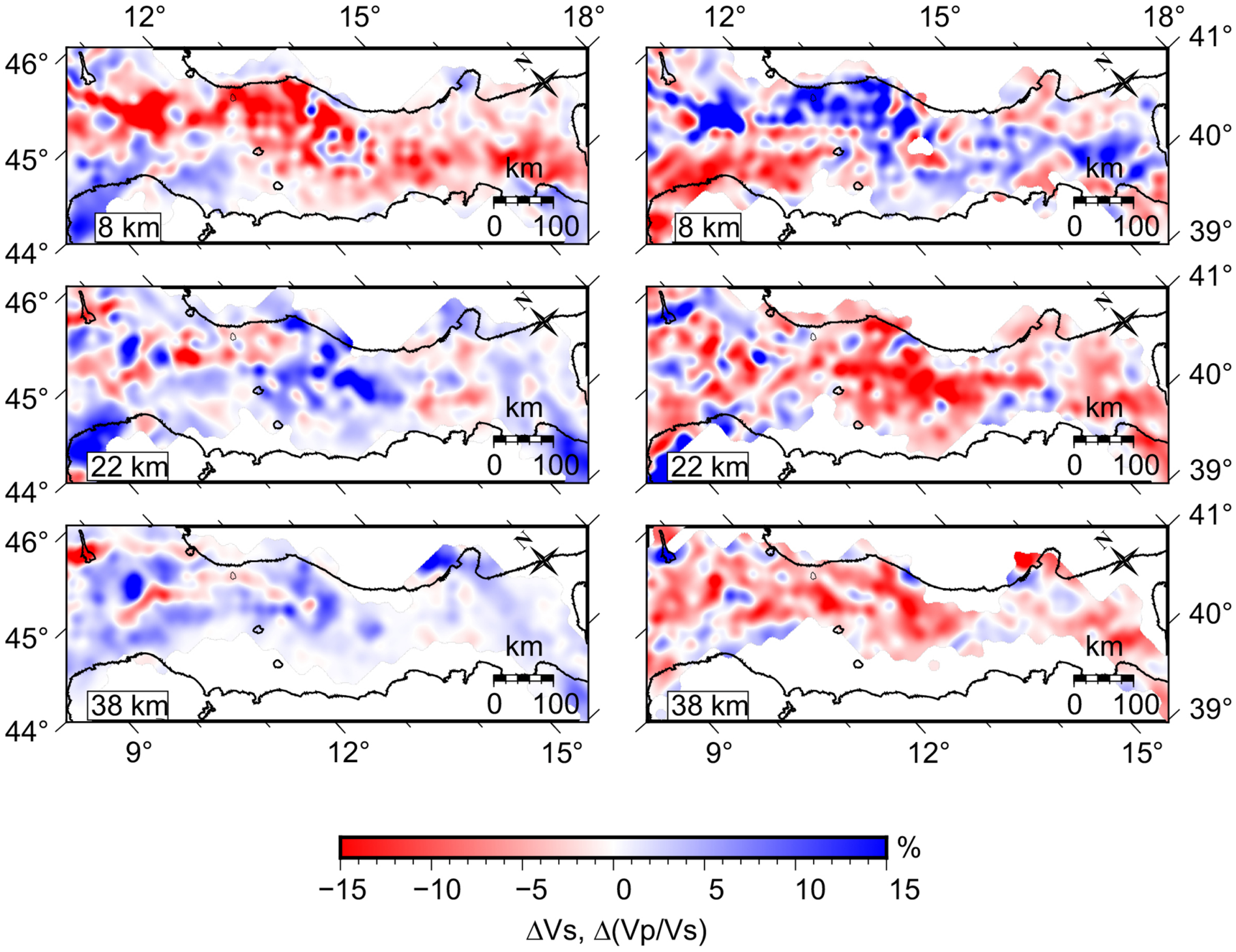
12°
15°
18°
46°
45°
44°
41°
40°
39°
8 km
22 km
38 km
km
0 100
9°
12°
15°
−15 −10 −5 0 5 10 15
%
ΔVs, Δ(Vp/Vs)

Figure 5

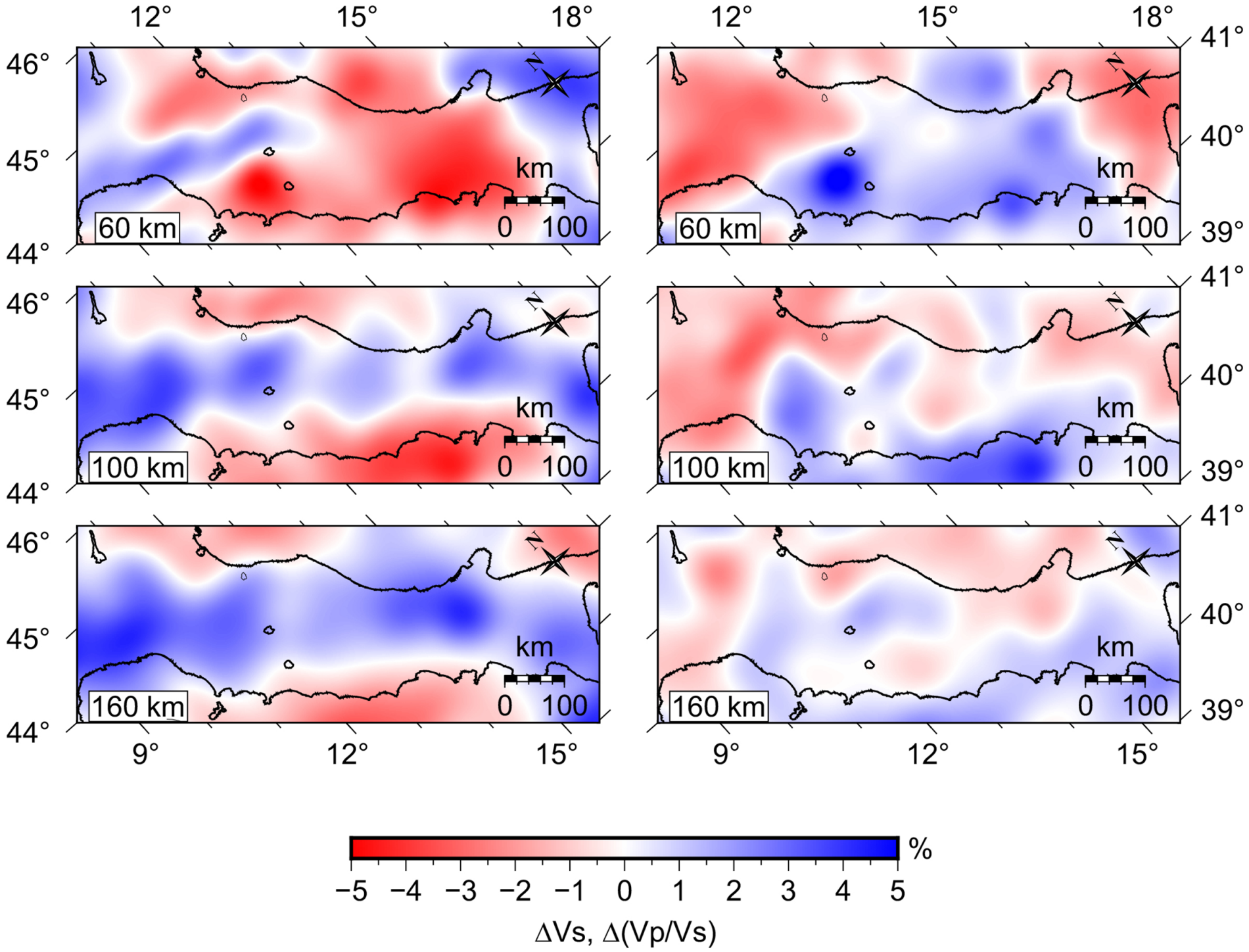
12°
15°
18°
46°
45°
44°
41°
40°
39°
9°
km
0 100
60 km
100 km
160 km
−5 −4 −3 −2 −1 0 1 2 3 4 5
%
ΔVs, Δ(Vp/Vs)

Figure 6

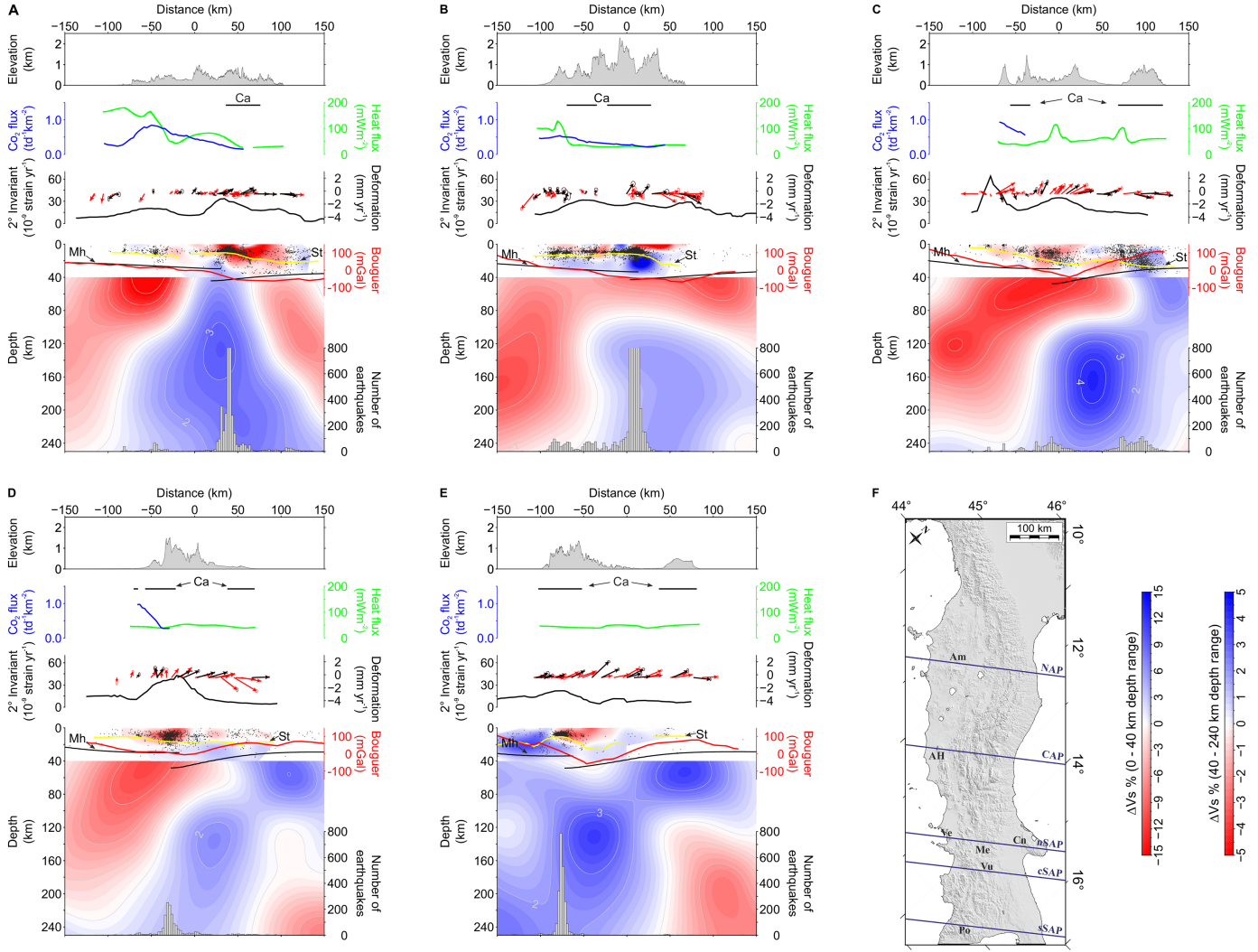
A
B
C
D
E
F
Distance (km)
Elevation (km)
Ca
Heat flux (mW/m²)
CO₂ flux (td⁻¹km⁻²)
2° Invariant (10⁻⁹ strain yr⁻¹)
Deformation (mm yr⁻¹)
Mh
St
Bouguer (mGal)
Depth (km)
Number of earthquakes
44°
45°
46°
10°
12°
14°
16°
100 km
Am
NAP
AH
CAP
Ve
Cu
nSAP
Me
Vu
cSAP
Fo
sSAP
ΔVs % (0 - 40 km depth range)
ΔVs % (40 - 240 km depth range)

Figure 7

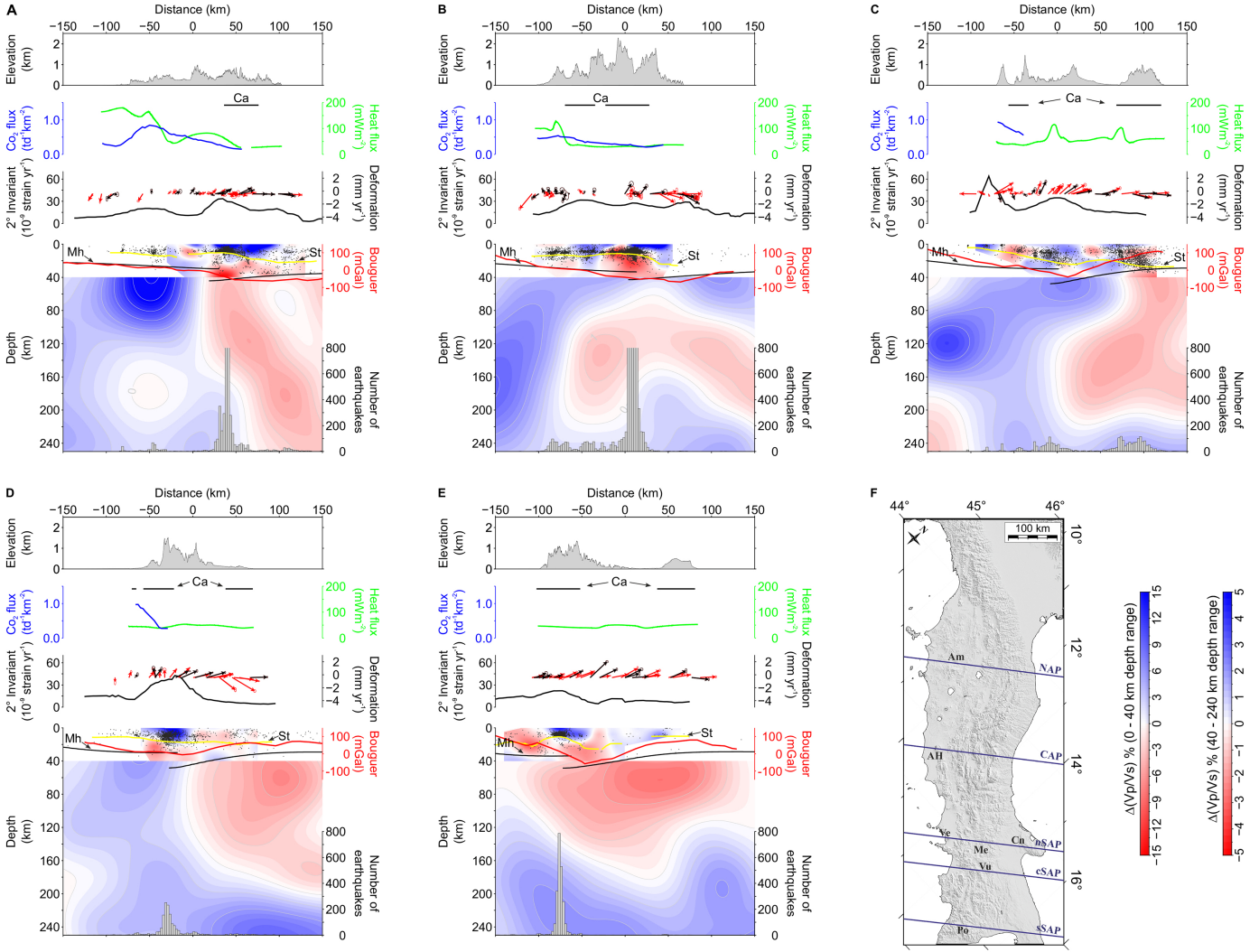
A
B
C
D
E
F
Distance (km)
Elevation (km)
Ca
Heat flux (mW/m²)
Deformation (mm yr⁻¹)
Mh
St
Bouguer (mGal)
Depth (km)
Number of earthquakes
44°
45°
46°
10°
12°
14°
16°
100 km
Am
NAP
AH
CAP
Ve
Cu
nSAP
Me
Vu
cSAP
Fo
sSAP
Δ(Vp/Vs) % (0 - 40 km depth range)
Δ(Vp/Vs) % (40 - 240 km depth range)

Figure 8